Machine Learning: Applications to GW data

Anupreeta More
(IUCAA)

IUCAA
Jan 6-10, 2025

Gravitational waves

Known waveforms Unknown waveforms

Short duration (~1s)

Long duration (∞)

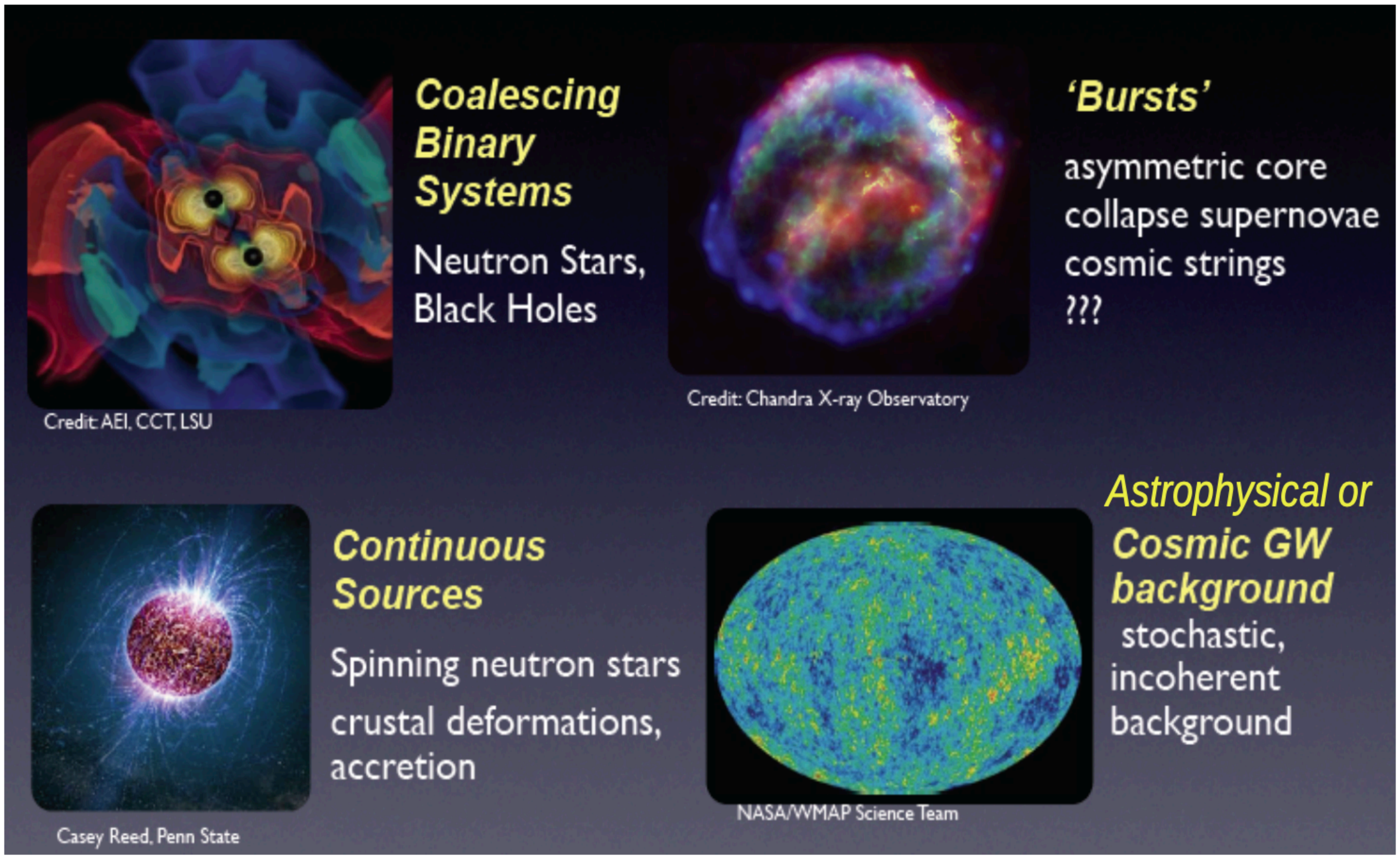

Courtesy: Marie Anne Bizouard

Compact Binary Coalescence

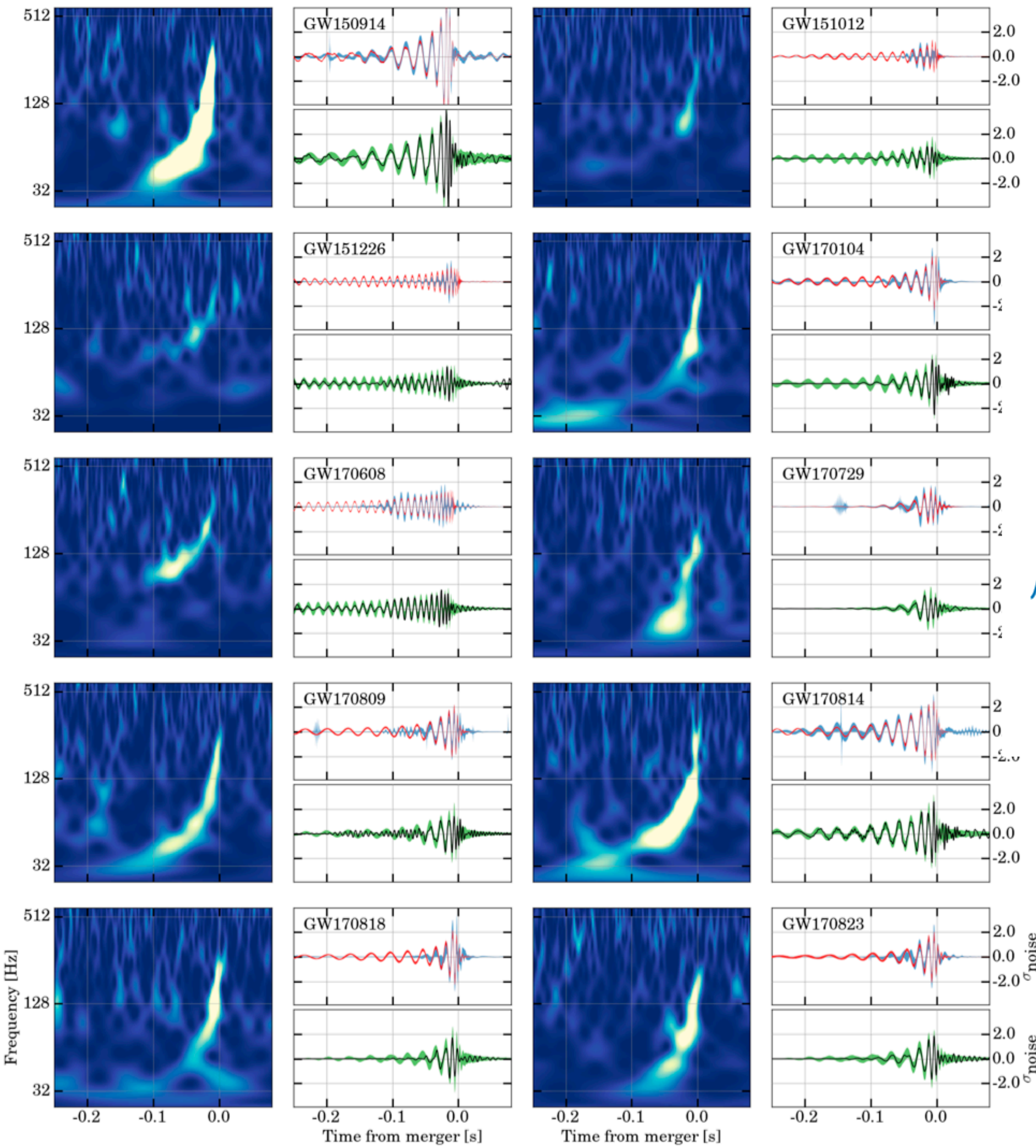

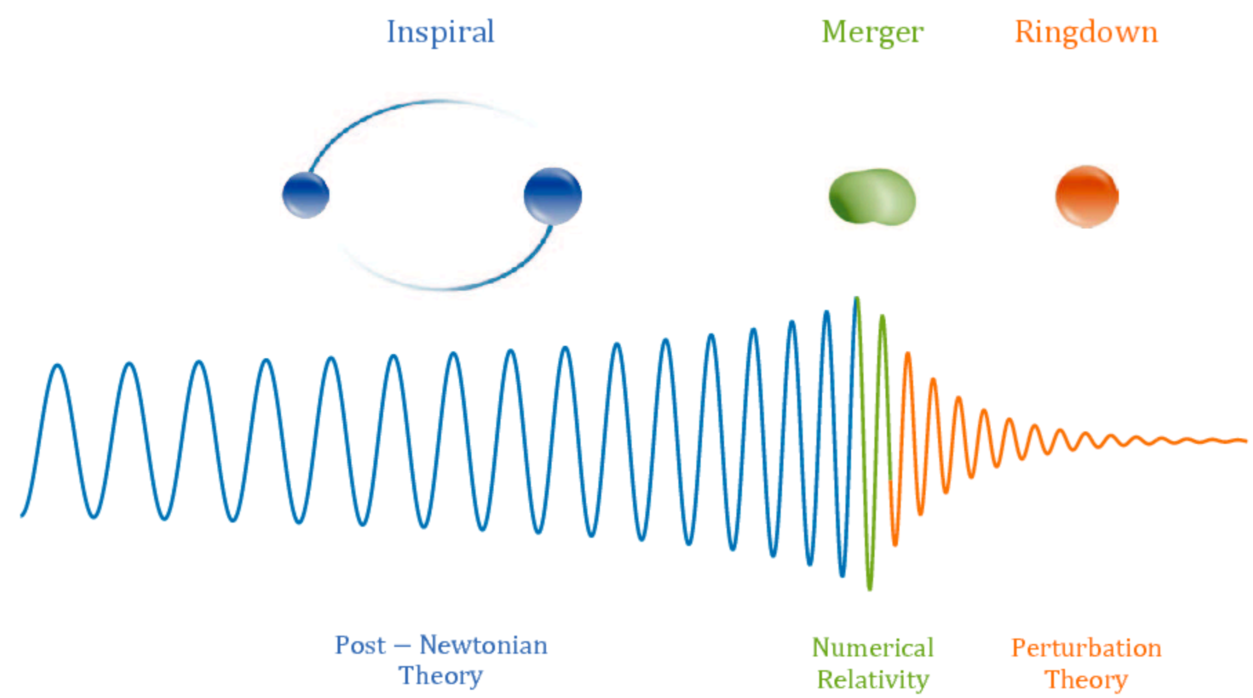

- GW signals detected from the mergers of
  - Binary Black Holes (BH) or
  - Binary Neutron stars (NS) or
  - NS-BH

Credit: LSC/Virgo, https://arxiv.org/abs/1811.12907

Glitches: Non-Gaussian Transient Noise

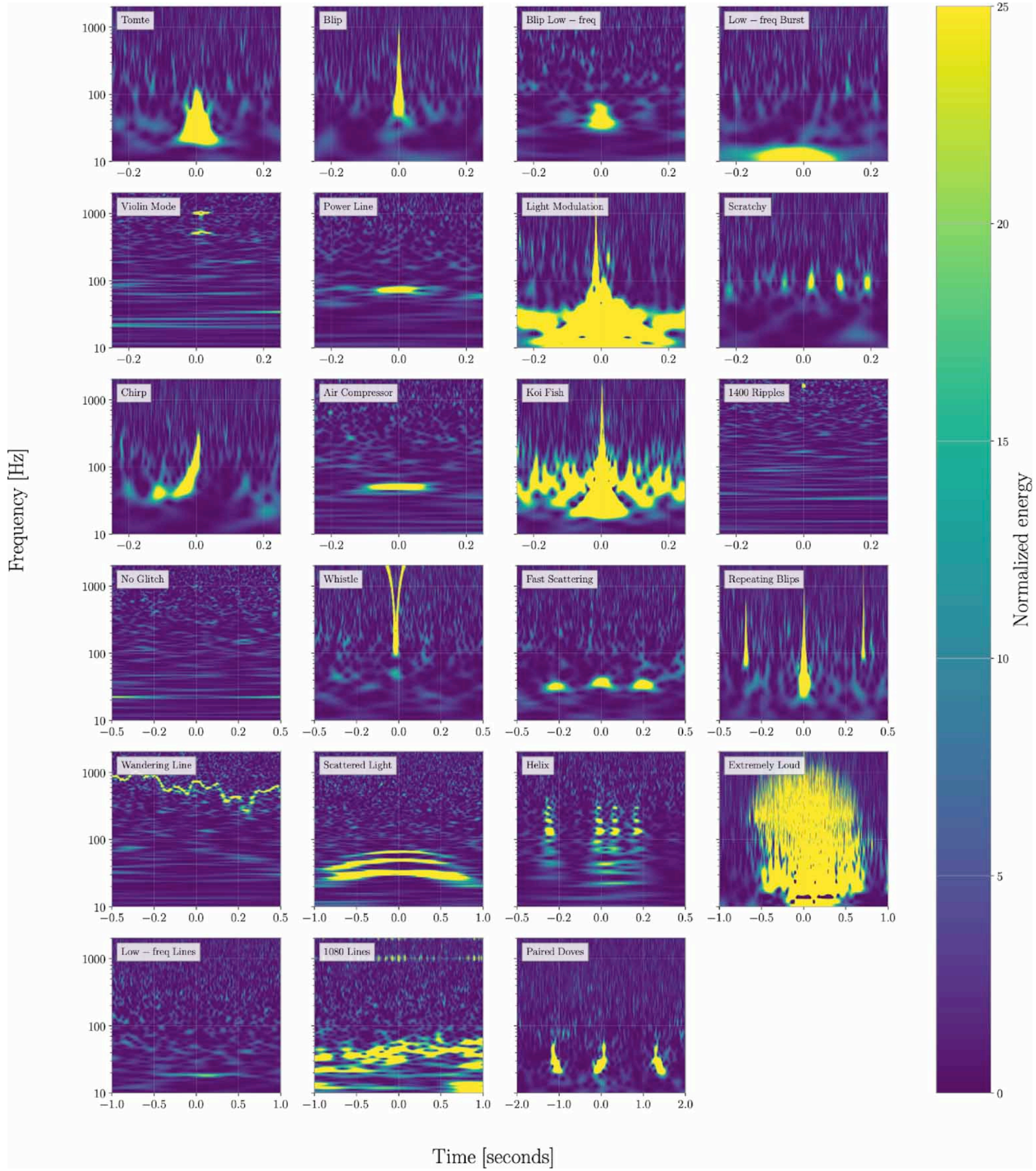

- Glitches are non-gaussian transient noise features
- Examples of different types of glitches found in the third observing run of LIGO data
- Glitches are of terrestrial origins but the cause of each type of glitch is not fully known and understood
- Some of the glitches have been persistent across many observing runs of LIGO

Credit: Glanzer et al. 2023

GW Searches

Matched Filtering

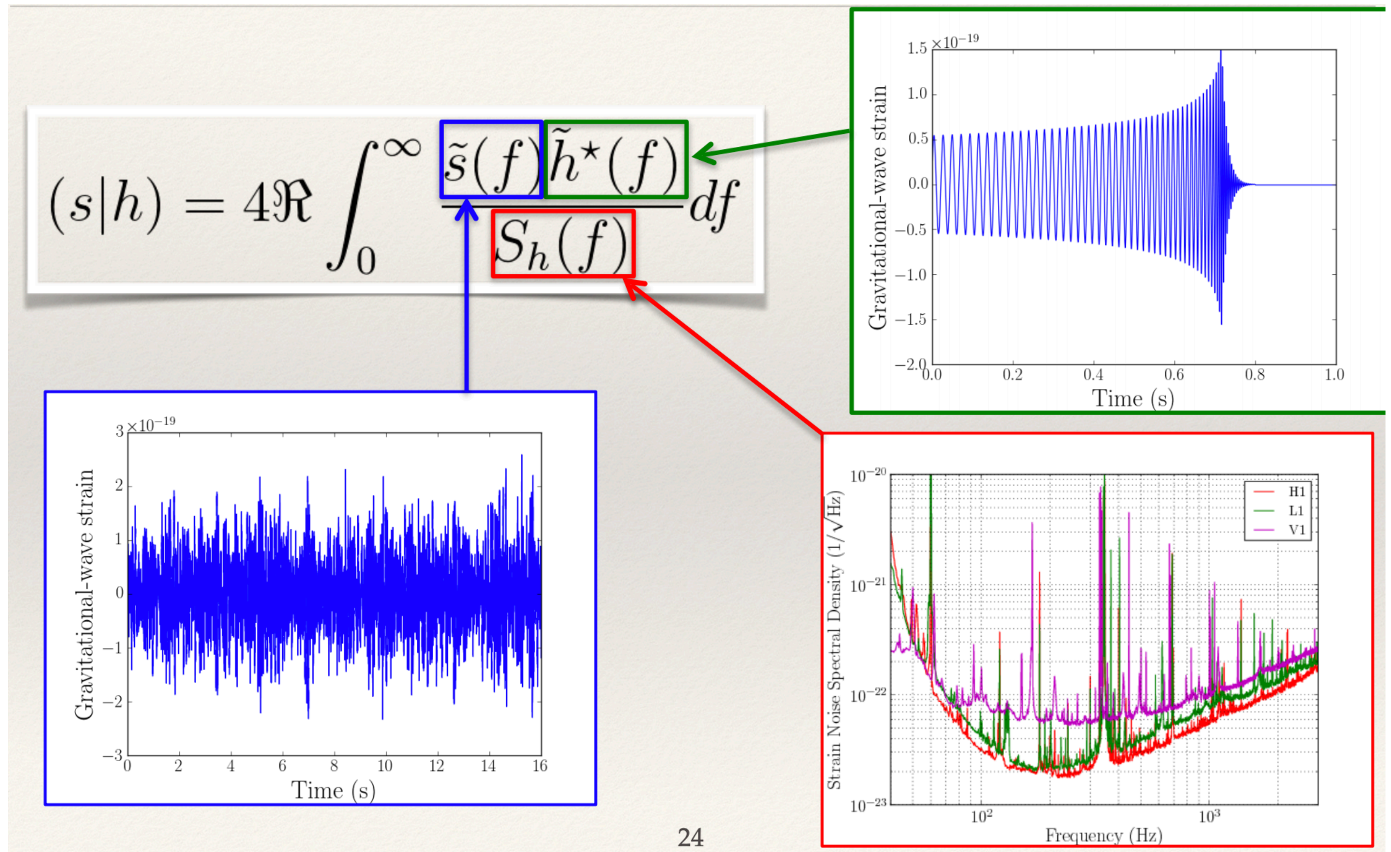

- MF is the primary technique for searching CBC signals and for model parameter estimation
- Signals depend on, at least, 15 model parameters and MF on >15D grid of waveforms is computationally expensive
- Simplifying assumptions are made to reduce the dimensionality during the actual search

Slide from I. Harry

Deep learning:
classification and parameter estimation

- Each training and test samples : 2500 BBH templates, M1(M2): 5 to 75 Msun mass
- Gaussian and real LIGO-like noise
- 1s sliding window, offsets of 0.2s
- Real LIGO data around 3 events used (training + testing)
    - found 0 false alarms and consistent GW event parameters

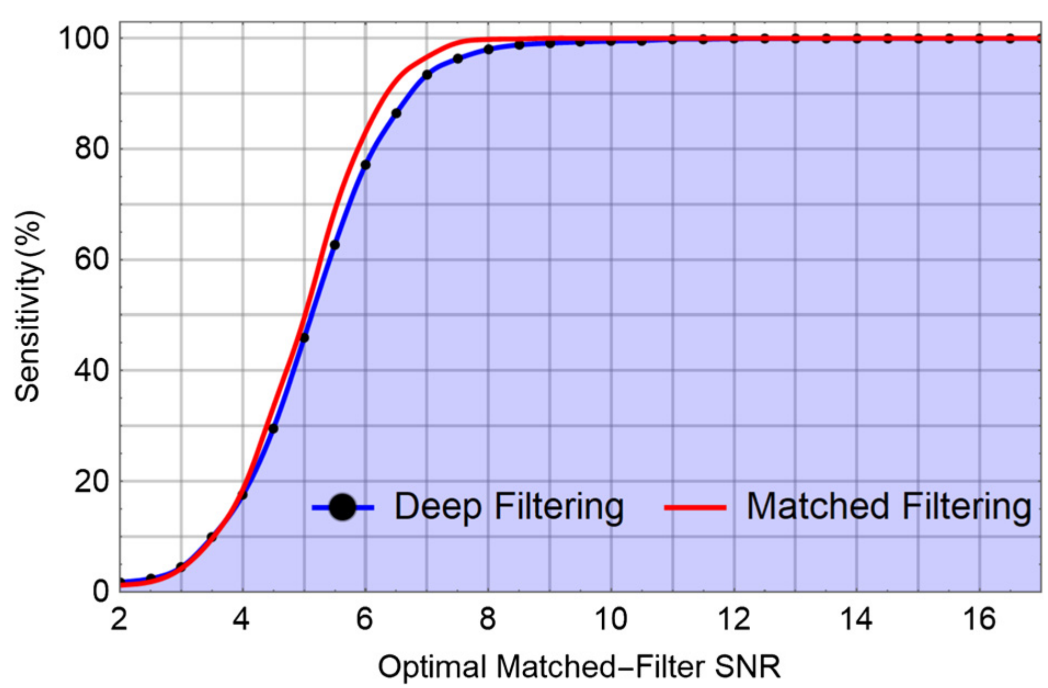

	Input	vector (size: 8192)
1	Reshape	matrix (size: 1 × 8192)
2	Convolution	matrix (size: 64 × 8177)
3	Pooling	matrix (size: 64 × 2044)
4	ReLU	matrix (size: 64 × 2044)
5	Convolution	matrix (size: 128 × 2014)
6	Pooling	matrix (size: 128 × 503)
7	ReLU	matrix (size: 128 × 503)
8	Convolution	matrix (size: 256 × 473)
9	Pooling	matrix (size: 256 × 118)
10	ReLU	matrix (size: 256 × 118)
11	Convolution	matrix (size: 512 × 56)
12	Pooling	matrix (size: 512 × 14)
13	ReLU	matrix (size: 512 × 14)
14	Flatten	vector (size: 7168)
15	Linear Layer	vector (size: 128)
16	ReLU	vector (size: 128)
17	Linear Layer	vector (size: 64)
18	ReLU	vector (size: 64)
19	Linear Layer	vector (size: 2)
	Output	vector (size: 2)

1D CNN for classification and PE tested on simulated and real GW events

George and Huerta 2018

Deep learning:
classification and parameter estimation

- Parameter estimation using ML comparable to MF
- Tested glitch contaminated signals
    - over 80% of the signals with SNR of 10 were detected, and their parameters estimated with less than 30% relative error,
- Tested detection of spin-precessing and eccentric BBH signals without prior training
    - with 100% sensitivity of detection and less than 35% error in estimating masses for SNR > 10

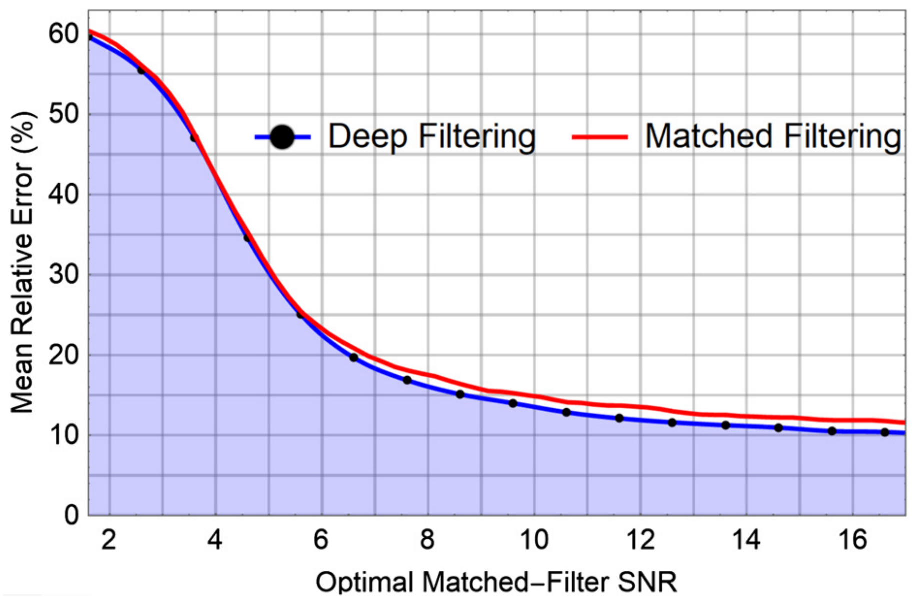

Computational speed

MF required over 2 s to analyze 1 s inputs.
In comparison, each of the CNNs took ~85 milli-sec and 540 micro-sec using a single CPU core and GPU respectively.

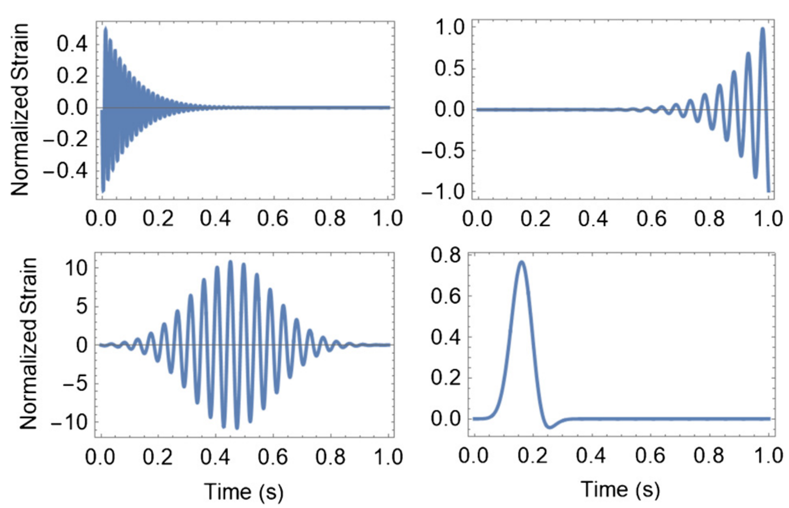

Artificial glitch like signals

George and Huerta 2018

SiGMAnet

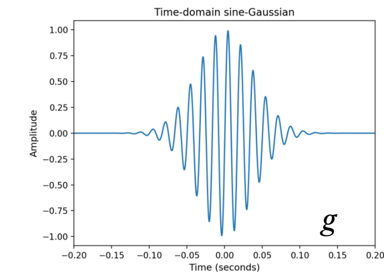

$$g(t) \equiv A e^{-4\pi f_0^2 \frac{(t-t_0)^2}{Q^2}} \cos(2\pi f_0 t + \phi_0) \,,$$

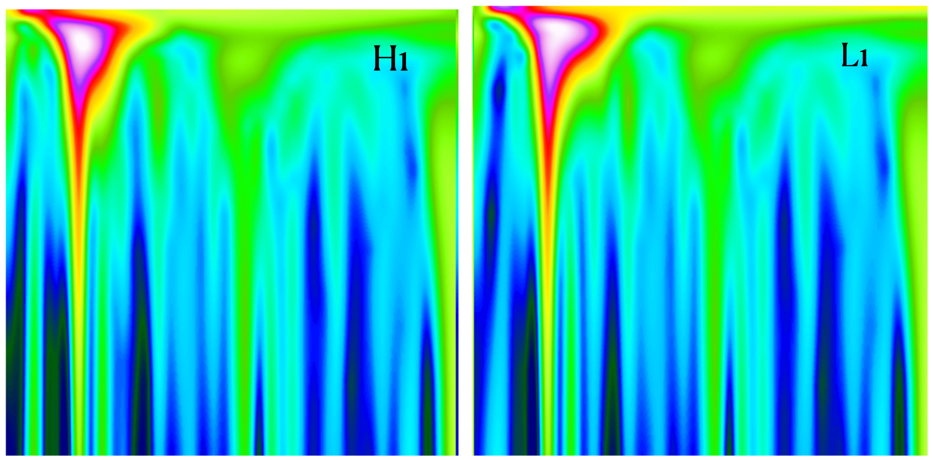

Projection of simulated BBH on SG (for H1 and L1)

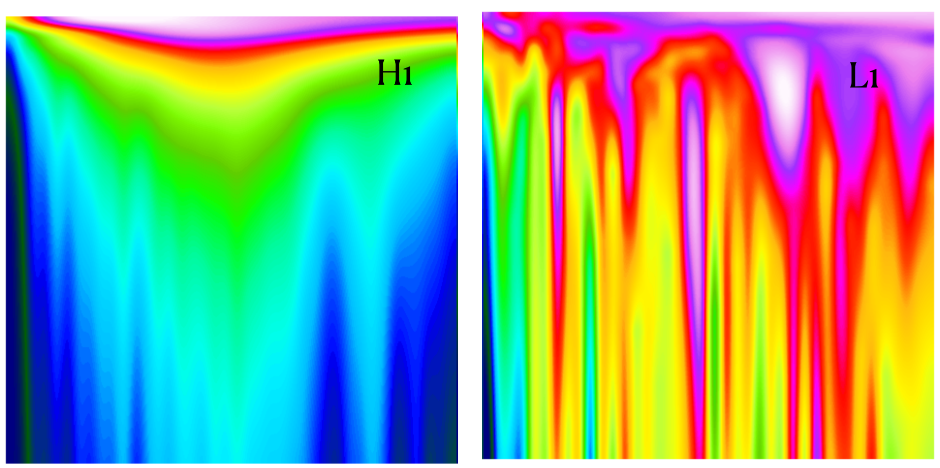

Projection of real Blip glitch on SG (for H1 and L1)

- Sine-Gaussian Projection (SGP) maps : Cross-correlation of the signal with Sine-Gaussian at varying Q and f_0
- Input data: SGP maps of simulated BBHs and real Blip glitches
- True astrophysical signals show similar projections in both detectors contrary to the glitches

- *CNN model* is trained on semi-simulated sample and tested on real data
- 95% of the GWTC-3 events are correctly identified
- GW170817, known to have a strong glitch in one of the detectors, was mis-identified to be a blip glitch

Choudhary, AM et al. 2022

SiGMAnet

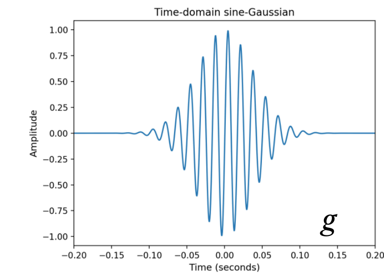

$$g(t) \equiv A e^{-4\pi f_0^2 \frac{(t-t_0)^2}{Q^2}} \cos(2\pi f_0 t + \phi_0)\,,$$

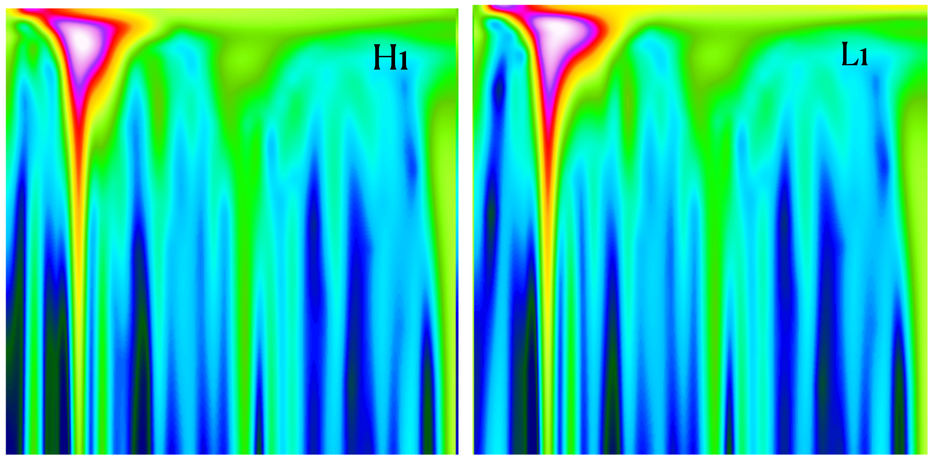

Projection of simulated BBH on SG (for H1 and L1)

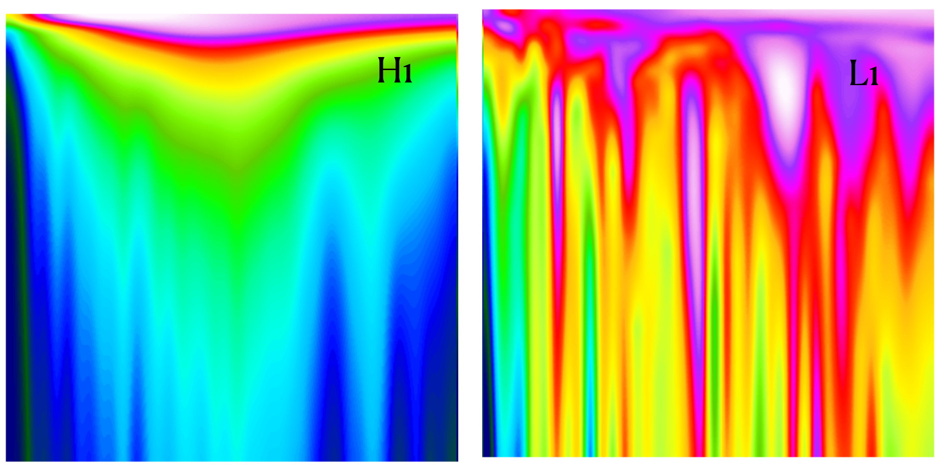

Projection of real Blip glitch on SG (for H1 and L1)

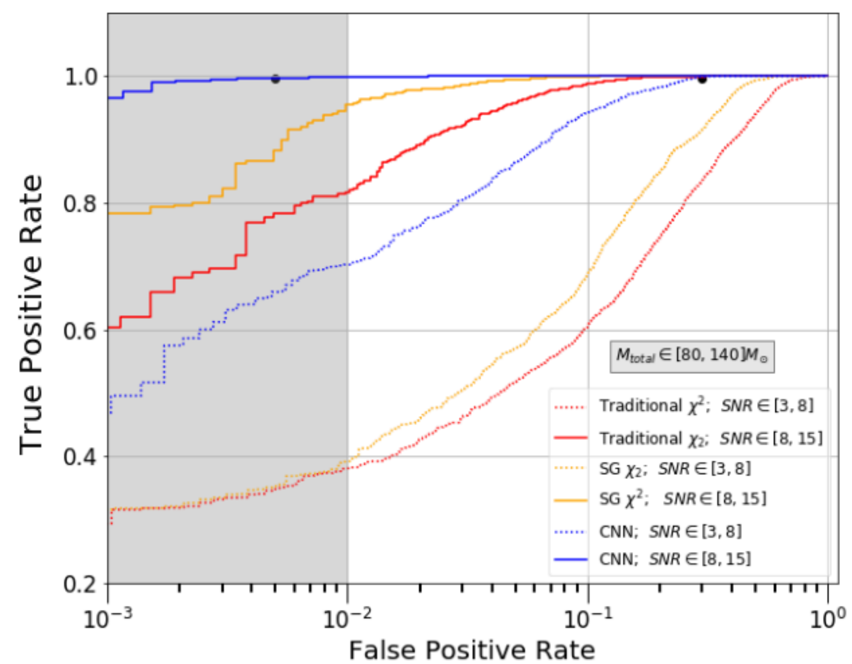

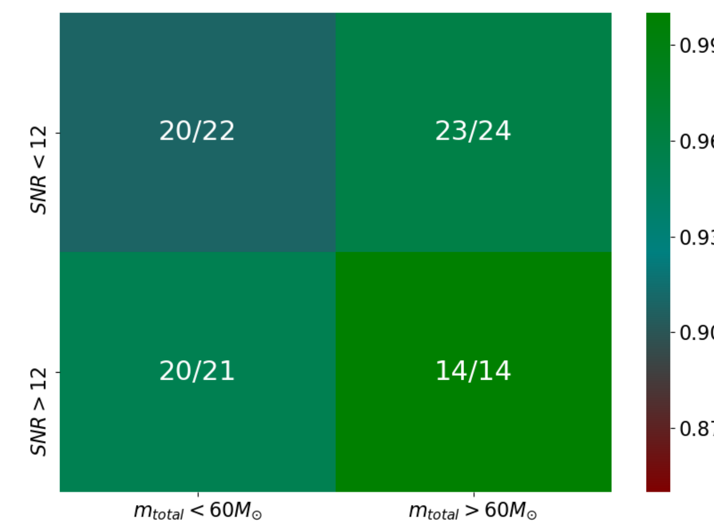

- Sine-Gaussian Projection (SGP) maps : Cross-correlation of the signal with Sine-Gaussian at varying Q and f_0
- Input data: SGP maps of simulated BBHs and real Blip glitches
- True astrophysical signals show similar projections in both detectors contrary to the glitches

- *CNN model* is trained on semi-simulated sample and tested on real data
- 95% of the GWTC-3 events are correctly identified
- GW170817, known to have a strong glitch in one of the detectors, was mis-identified to be a blip glitch

Choudhary, AM et al. 2022

AresGW

- Training : BBH (non-aligned spins) and real noise data segments
    - each of duration 1.25sec
    - each of sample size 740k
- Data preprocessing - DAIN

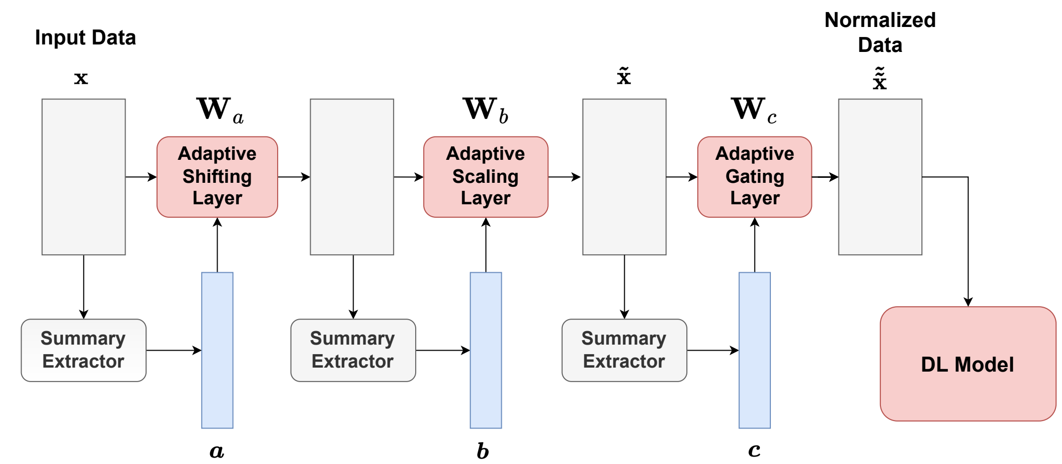

Deep Adaptive Normalization (DAIN)

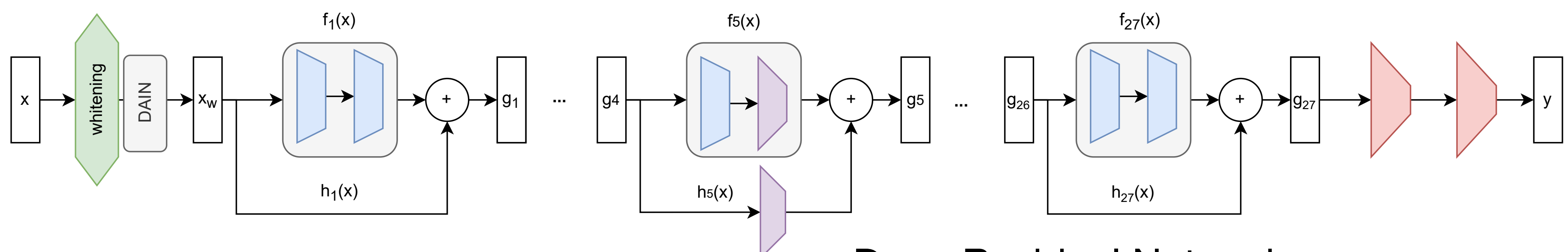

Deep Residual Network

- Deep Residual Network (54-layer) along with dynamic augmentation and curriculum learning
- Comparison with traditional BBH searches

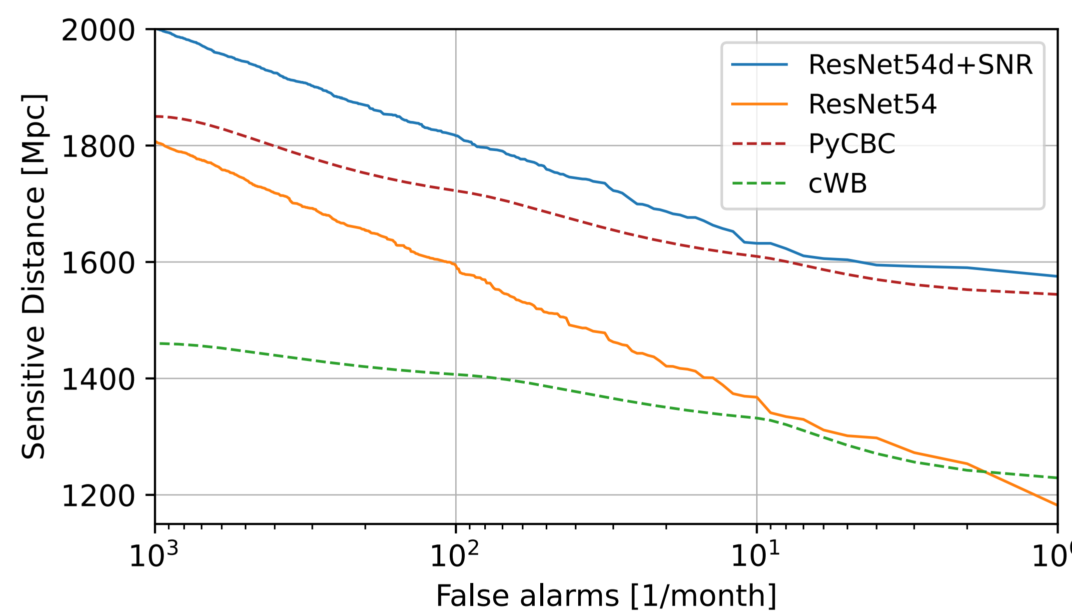

Mock data challenge - Schaefer et al. (2023)

Nousi et al. (2023), Koloniari et al. (2024)

Noise characterization

Gravity Spy: CNN + Citizen Science

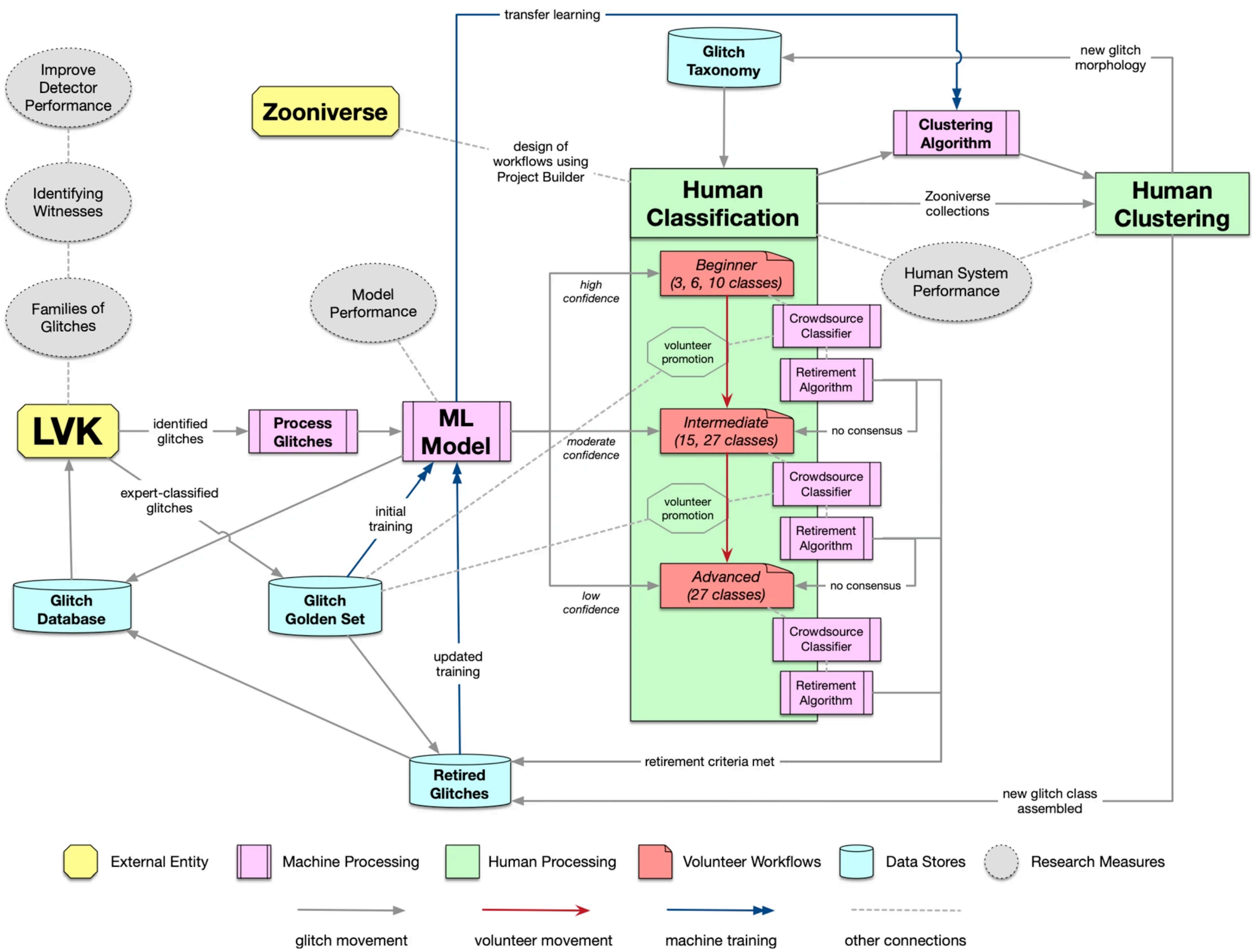

Zevin et al. 2024

- 10^5 glitches from O1 (Omicron SNR>7.5, 10 Hz < glitch peaks< 2048 Hz, unflagged data)
- Then known 3 real events were excluded but simulated GW events were added to the real data
- Preliminary ML trained on 100 glitches/ class identified by humans
  - Training set: 7718 glitches, 20 classes
- ML trained glitches are characterized by G. Spy

Zevin et al. 2017

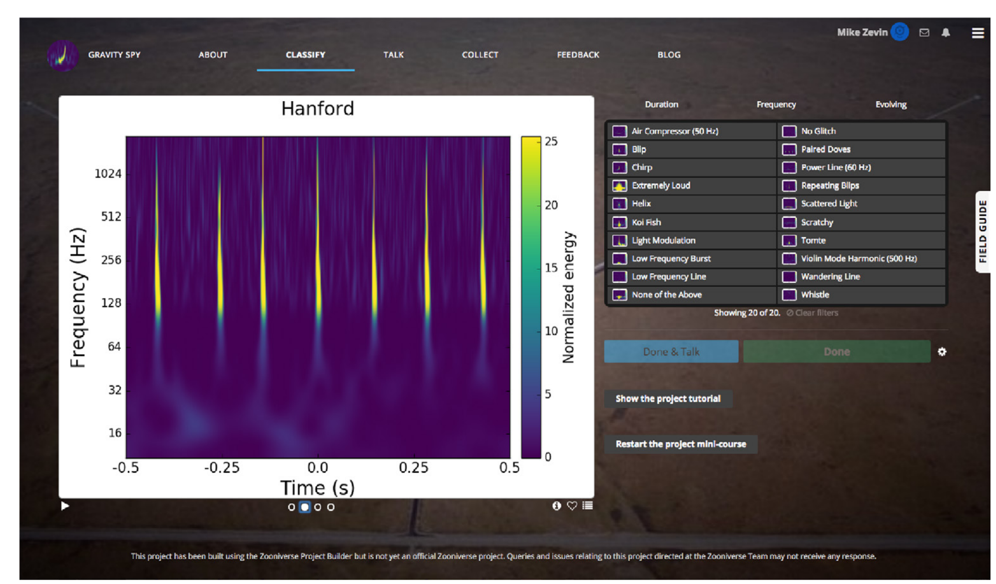

Figure 3. Gravity Spy user interface. This image shows the *black hole merger* workflow (see section 3.2.3), with all 20 currently designated categories as options.

Table 3. Classification accuracy of single and multi-view CNNs.

Classifier	Accuracy (%)
The best single view model	95.34
parallel view model	95.75
merged view model	**96.89**

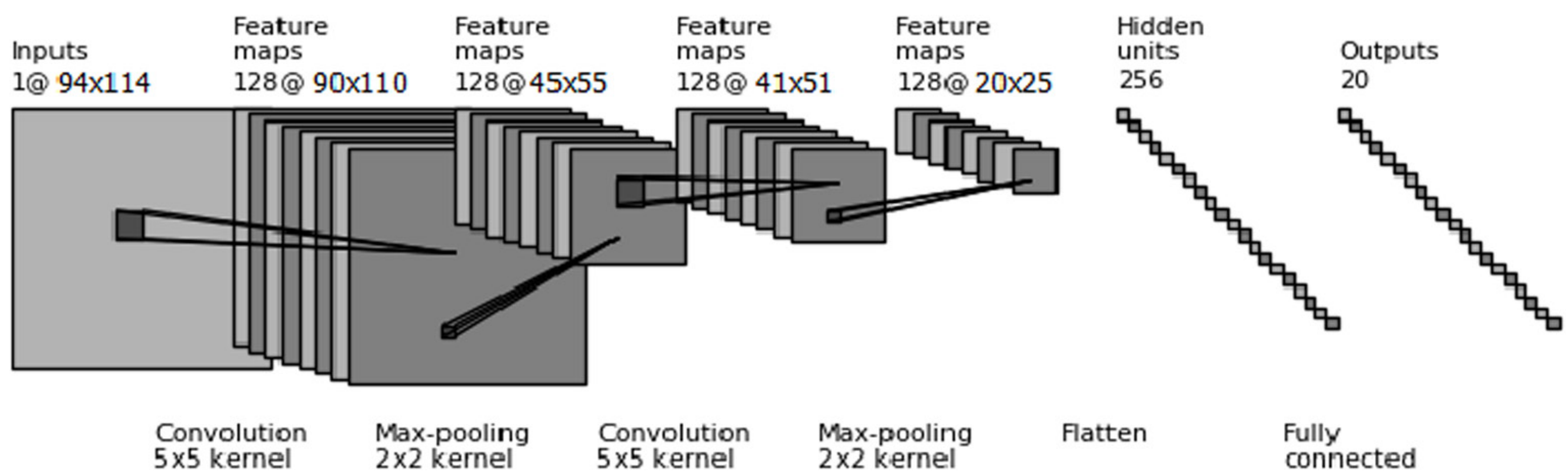

Parallel view

Merged view

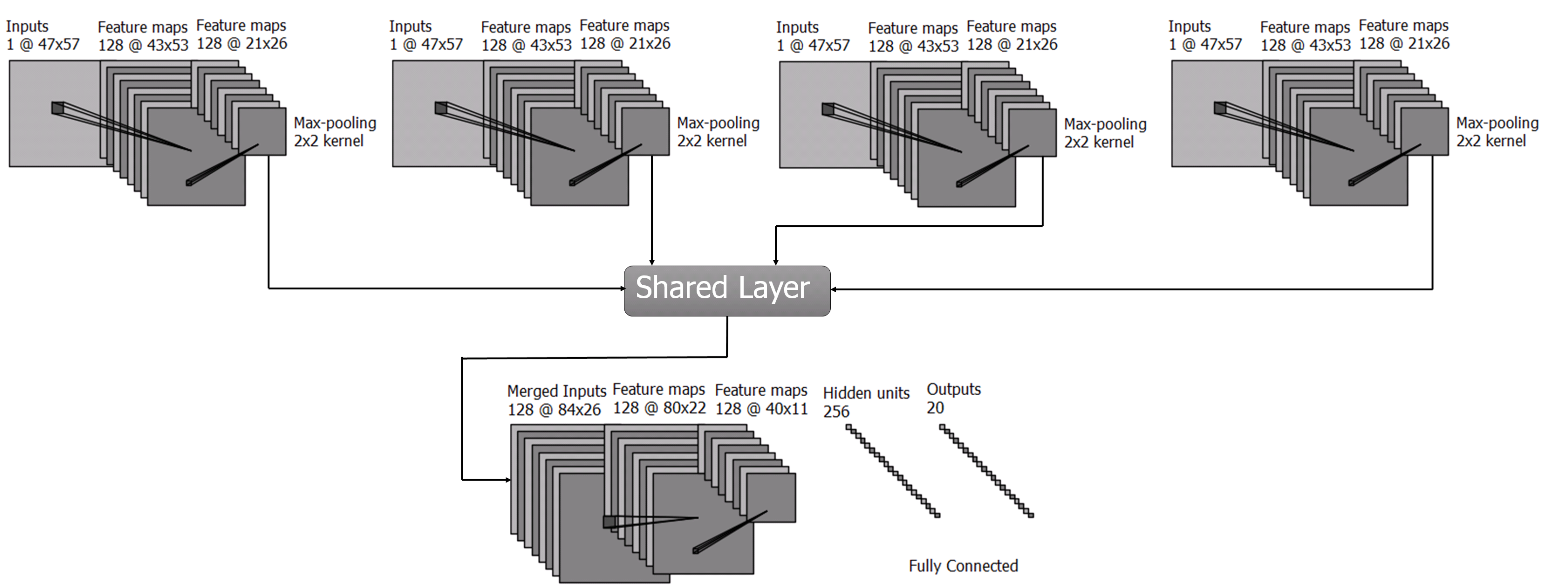

Bahaadini et al. 2017

Zevin et al. 2017

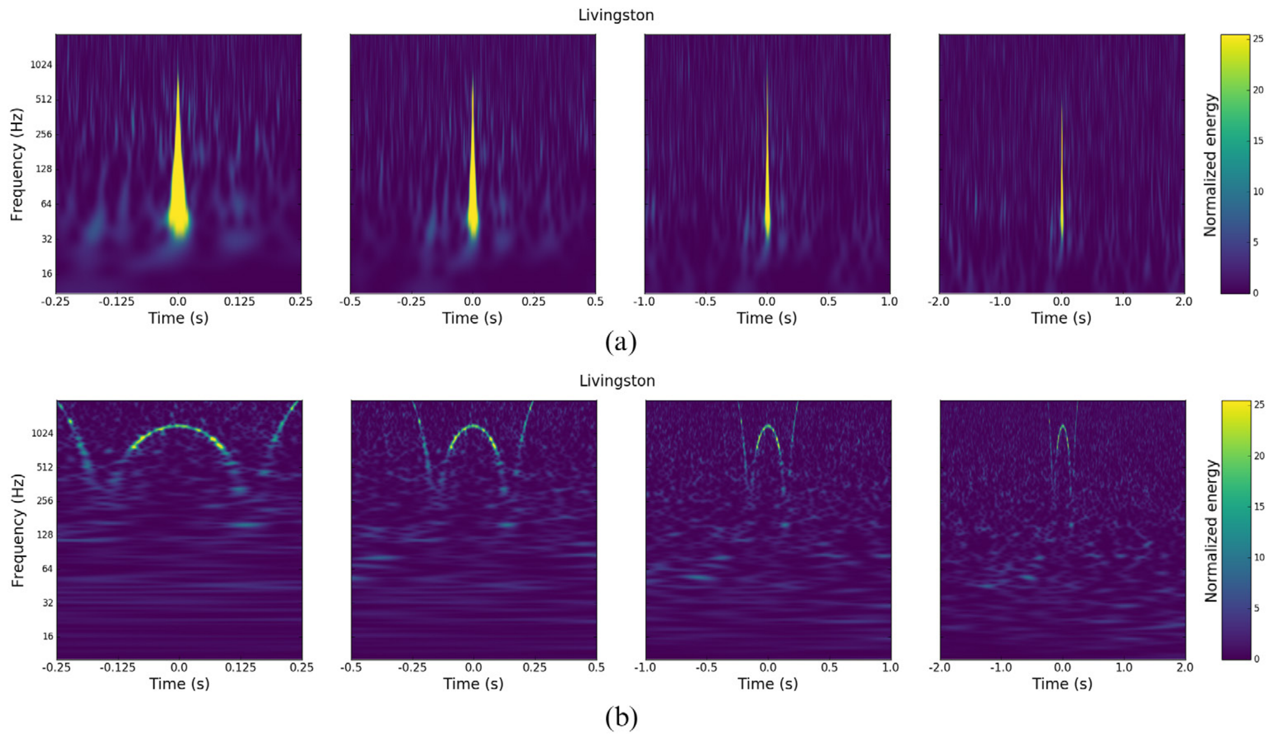

Table 3. Classification accuracy of single and multi-view CNNs.

Classifier	Accuracy (%)
The best single view model	95.34
parallel view model	95.75
merged view model	**96.89**

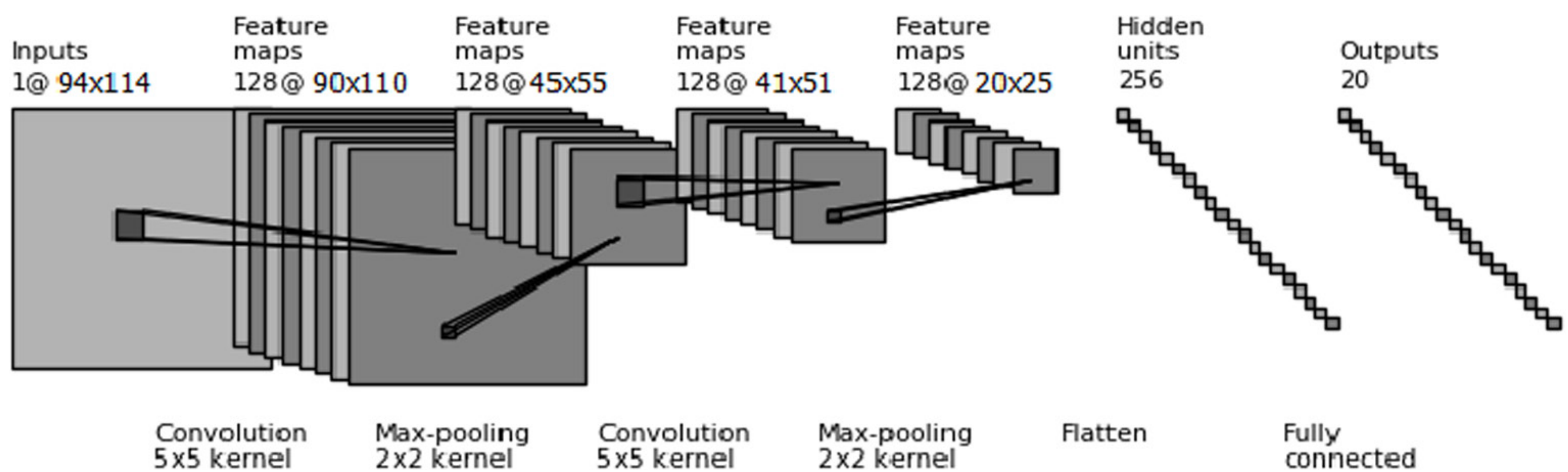

Merged view

Parallel view

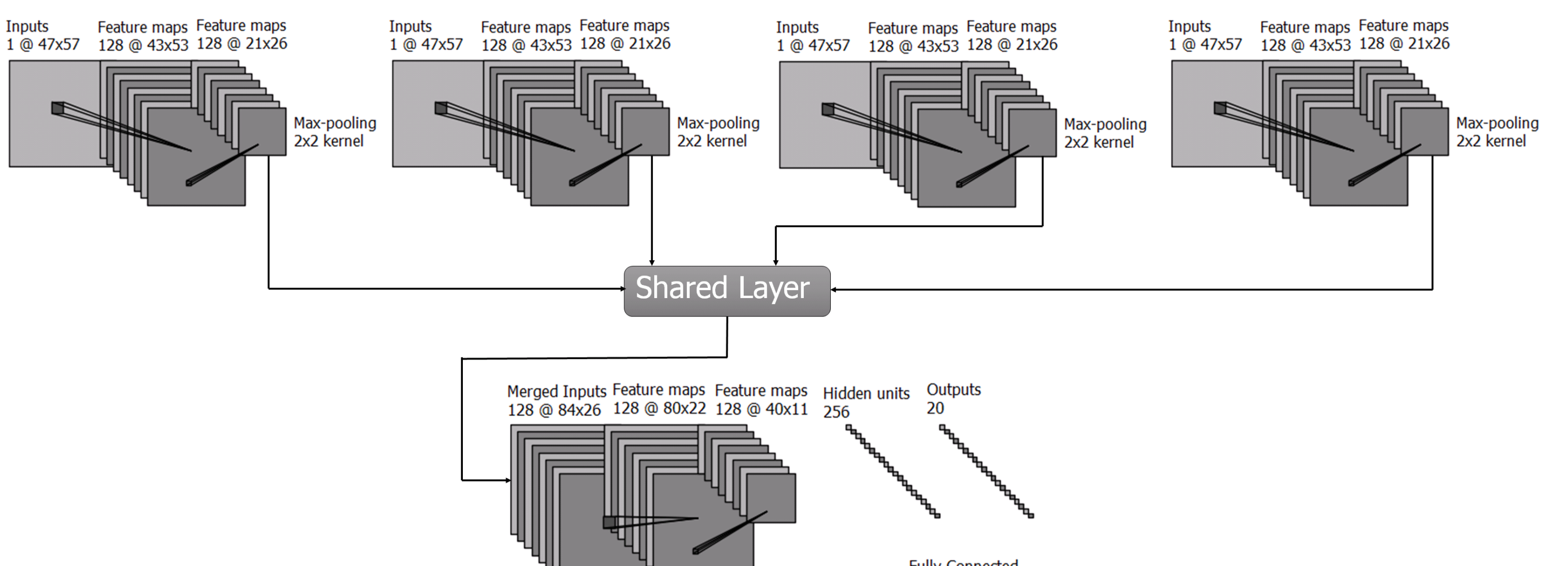

Bahaadini et al. 2017

Zevin et al. 2017

Gravity Spy: CNN + Citizen Science

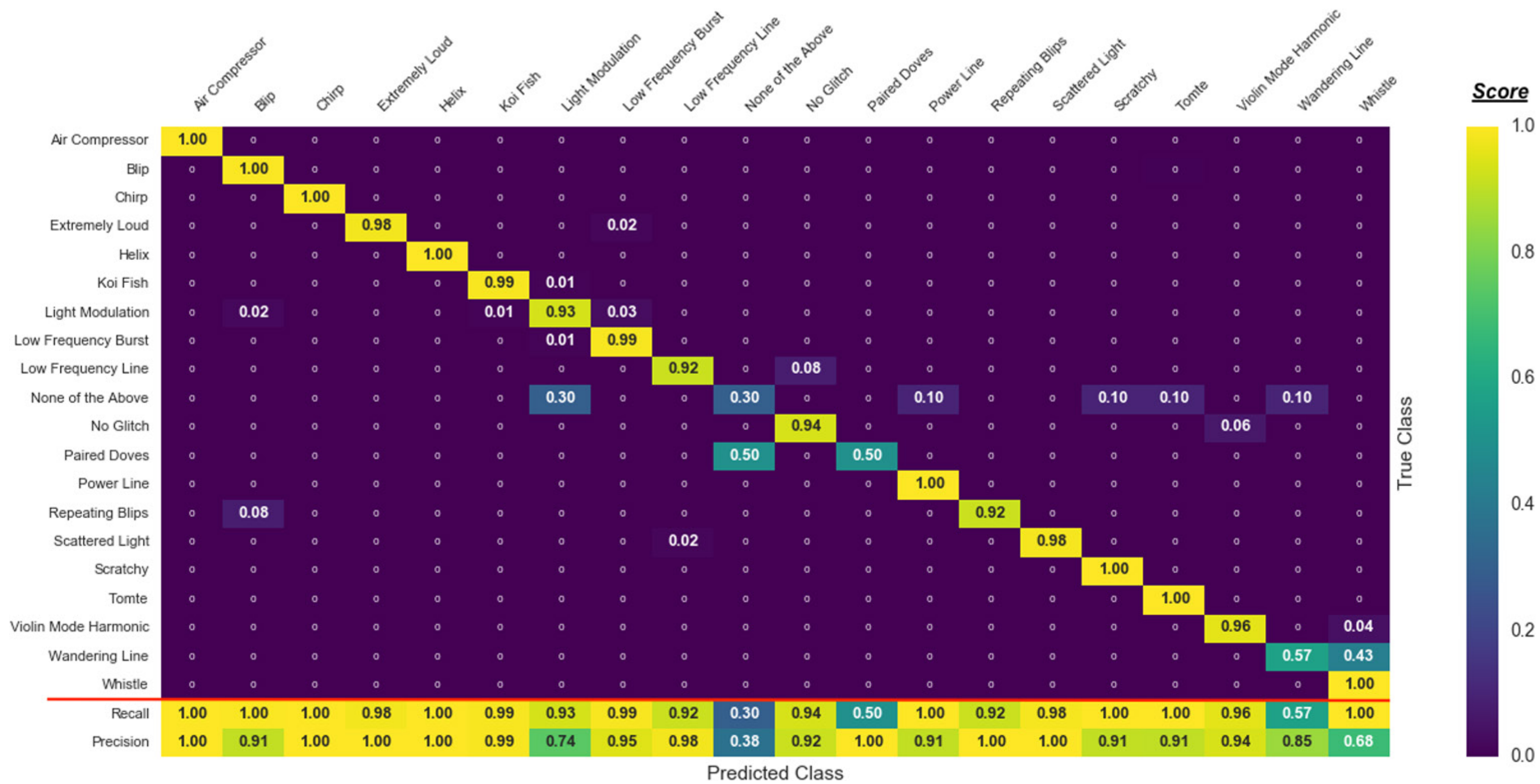

ML learning performance

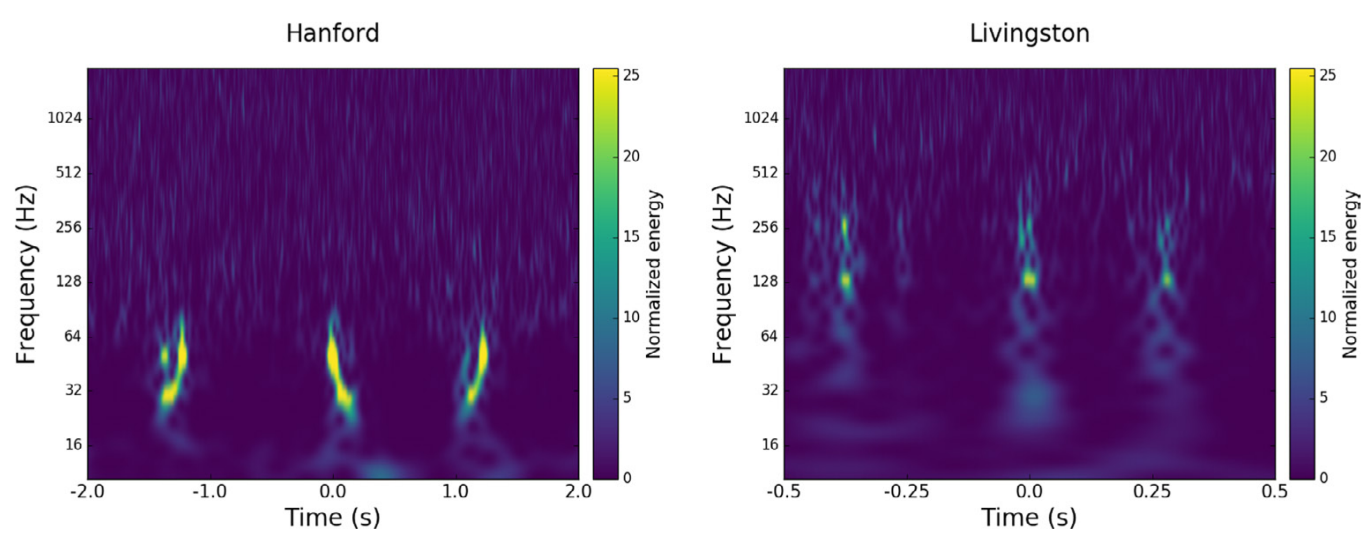

Paired Doves (L) and Helix (R). Two new classes of glitches identified during the beta testing of Gravity Spy

Zevin et al. 2017

Characterizing Glitches with environmental data

- Auxiliary channels monitor the state of the various subsystems of the IFO (e.g. suspensions, optics, seismic)
- Glitch identification and tracking their origins can be efficient through aux channels

- 40,000 aux only channels are used
- Input data is a vector of 10 parameters that capture the statistical behavior of each timestamp (7500 glitches and 7500 glitch-free)
- The best model with Acc=0.84 has features which mainly came from 56 aux channels

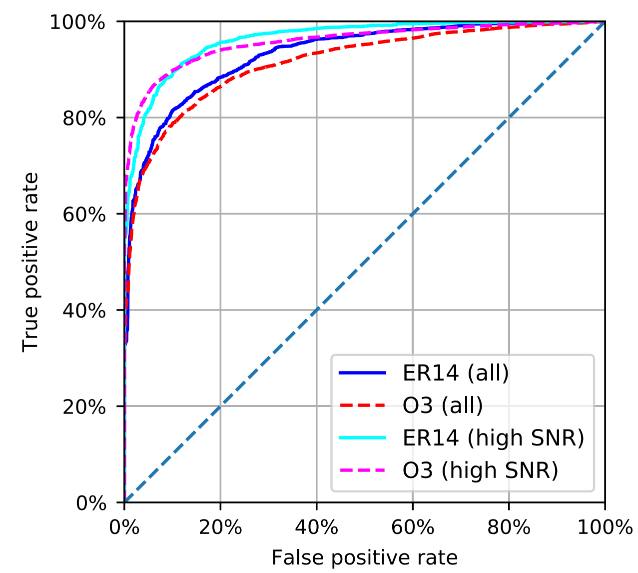

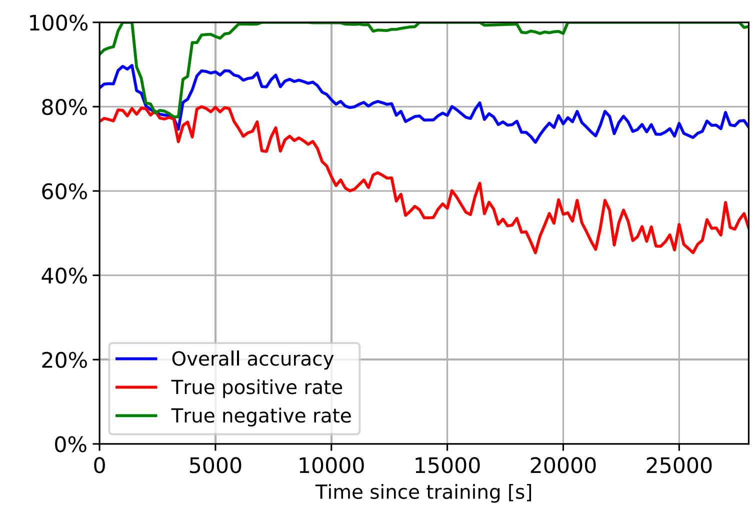

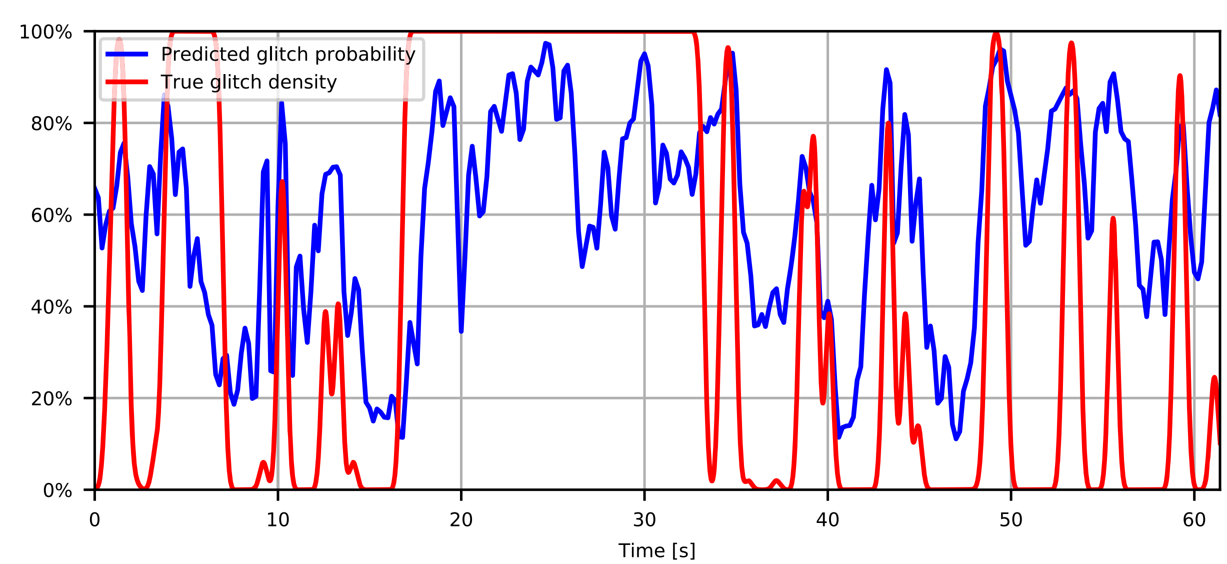

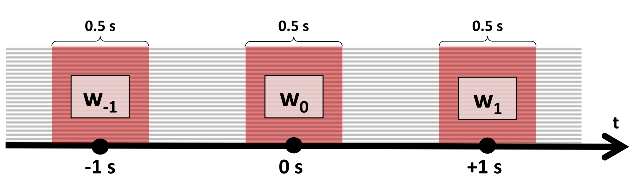

Colgan et al. 2020

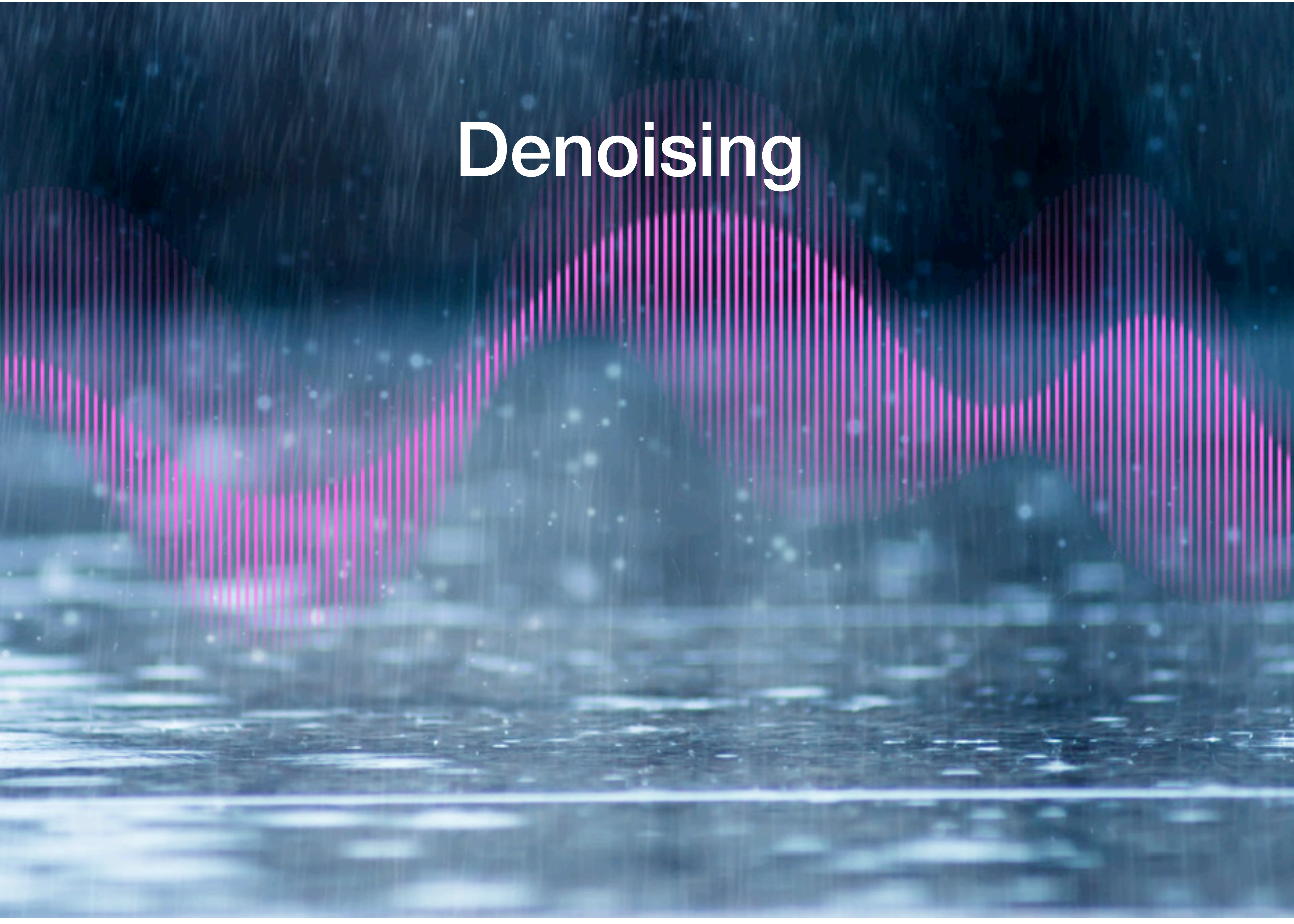
Denoising

Denoising AutoEncoders I

- Simple CNN-Denoising AE applied
- Training sample has simulated signals injected in real LIGO noise and real glitches
    - sample sizes are small (about 7K+1K)
- Real GW Signals are recovered with good overlap with injected signals and comparable SNRs
- Faster training and suitable for searching in low latency

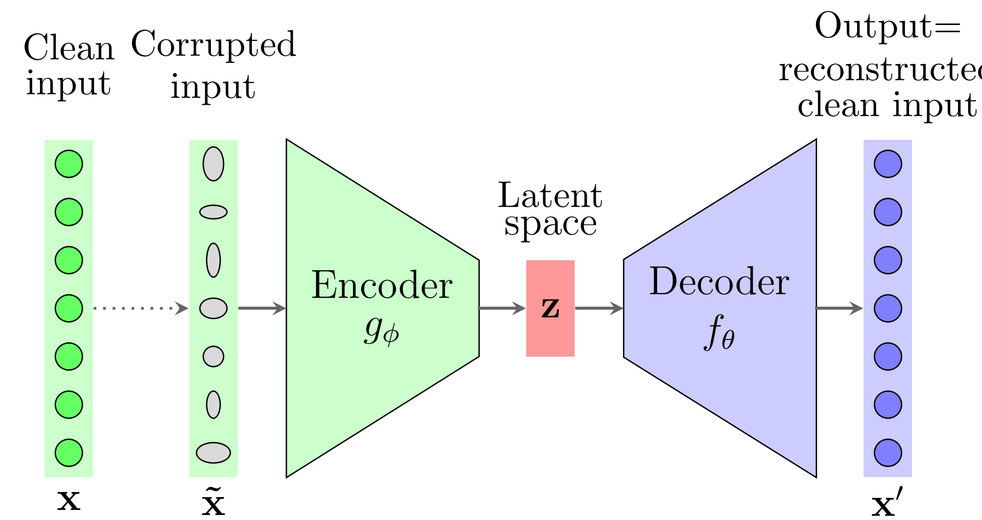

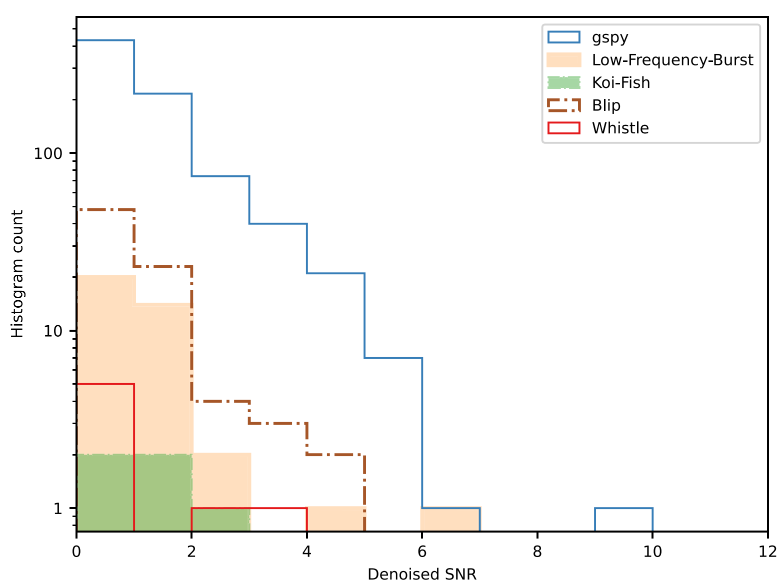

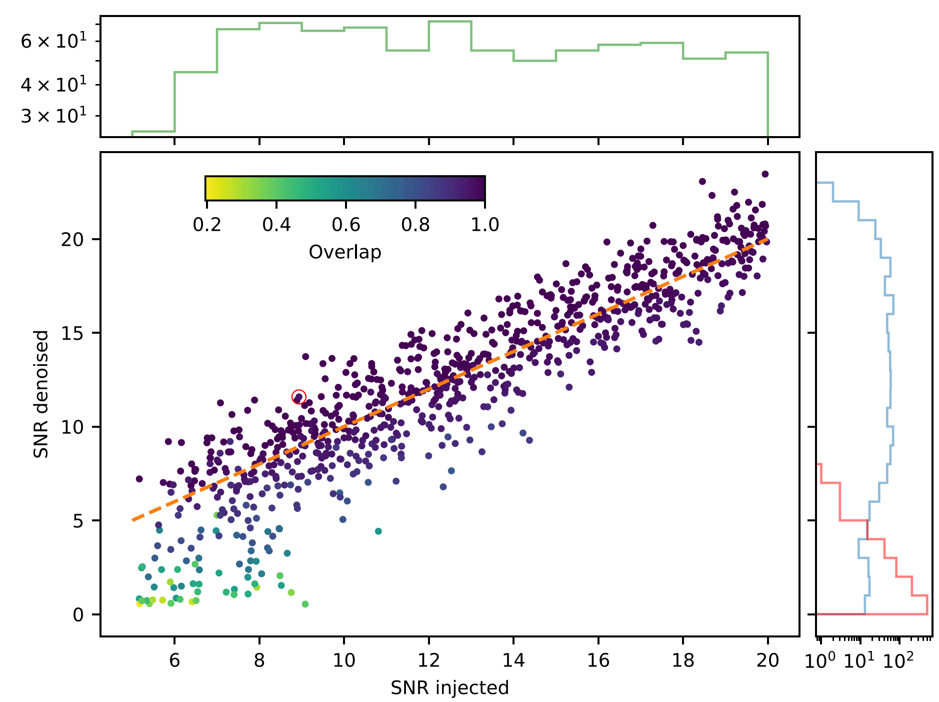

Bacon et al. 2023

Denoising AutoEncoders II

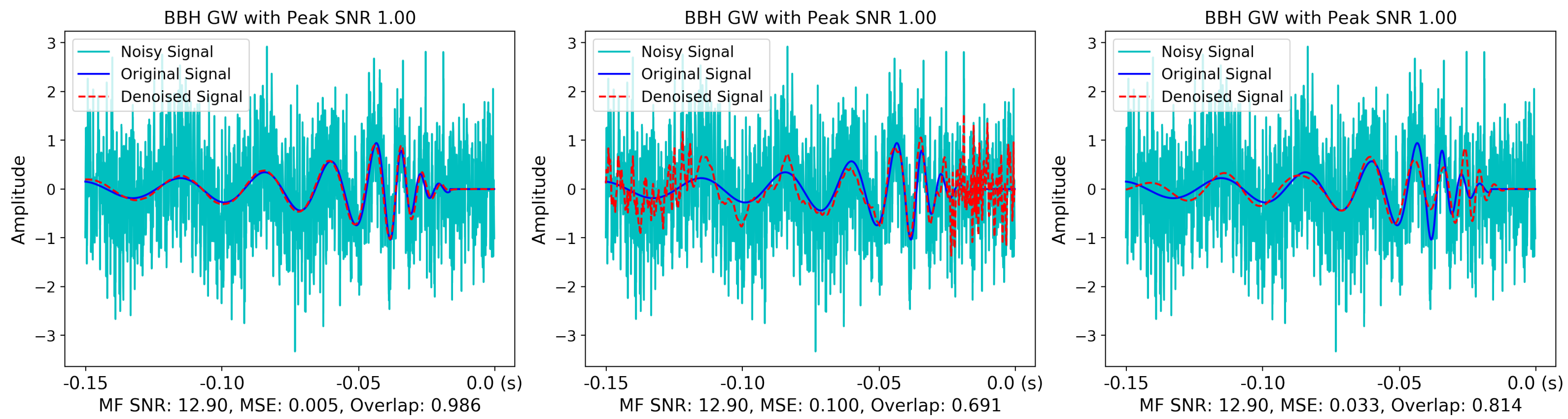

(a)SMTDAE (b)Dictionary Learning (c)PCA

- Combines DAE with Recurrent NN in a new algorithm called Staired Multi-timestep denoising AE (SMTDAE)
  - takes multiple time steps within the neighbourhood to predict the value of a specific point
- Trained on Signals injected in additive white Gaussian Noise
- Curriculum learning applied during training
- Demonstrated to work on test data with real LIGO noise and on GW signals with additional complexities (spinning, eccentricity)

Shen et al. 2017

Parameter Estimation

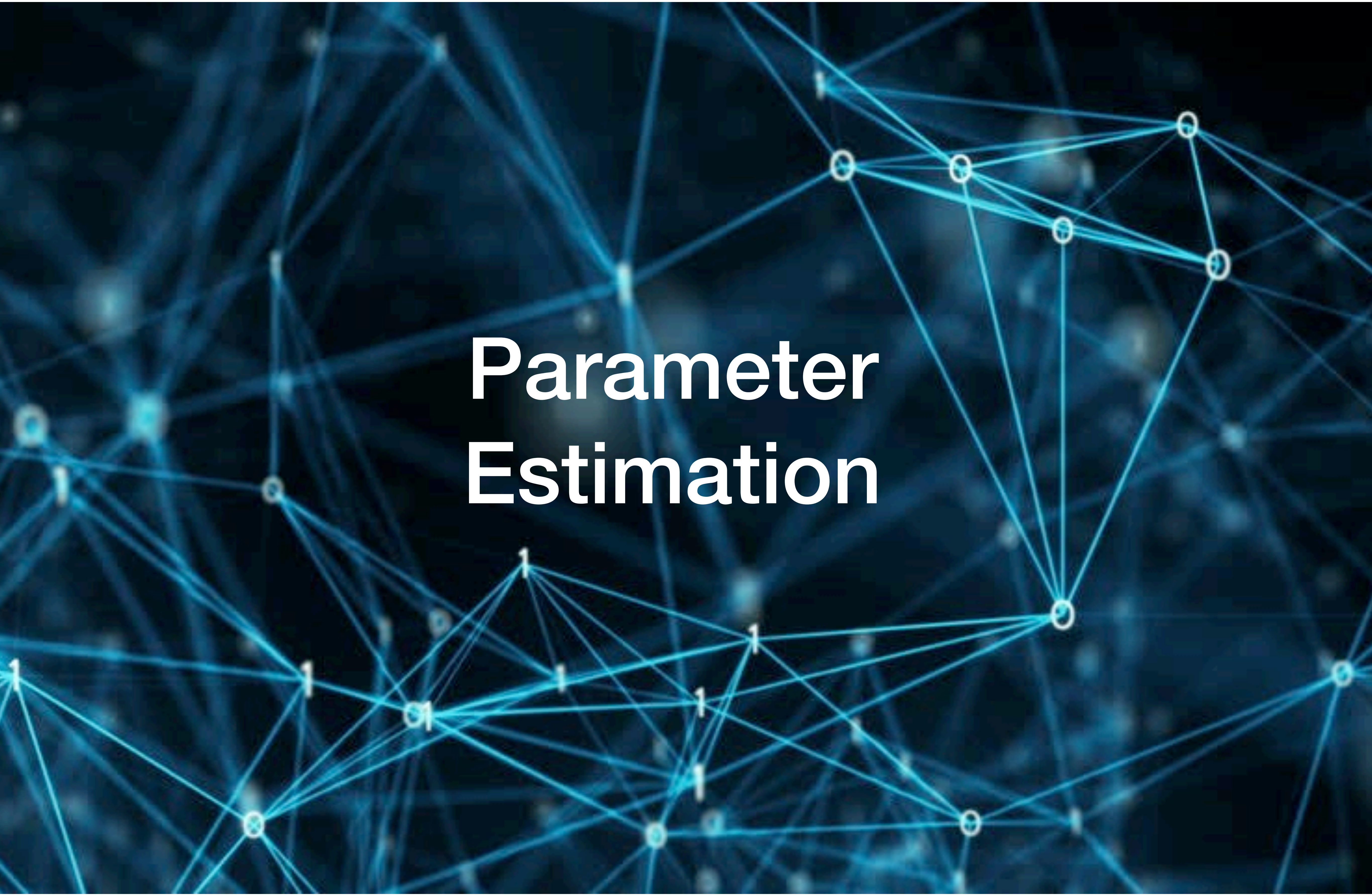

CBC model parameters

- **Intrinsic** parameters: primary and secondary **masses** and **spins** (and eccentricity)

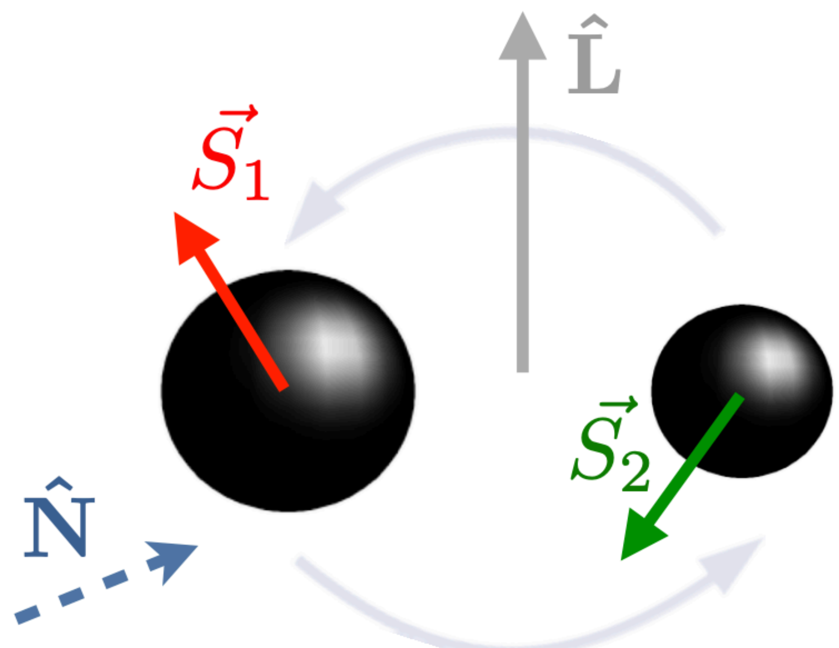

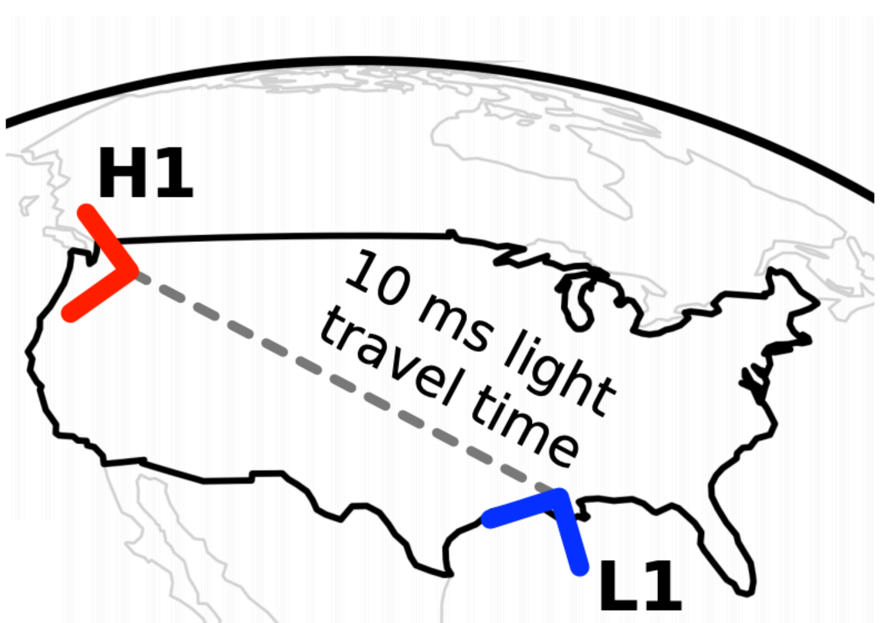

- **Extrinsic**: time, **sky-position**, distance, **orientation**, reference phase

Credit: LIGO/Virgo, Slide from V. Raymond

Parameter estimation with CVAE

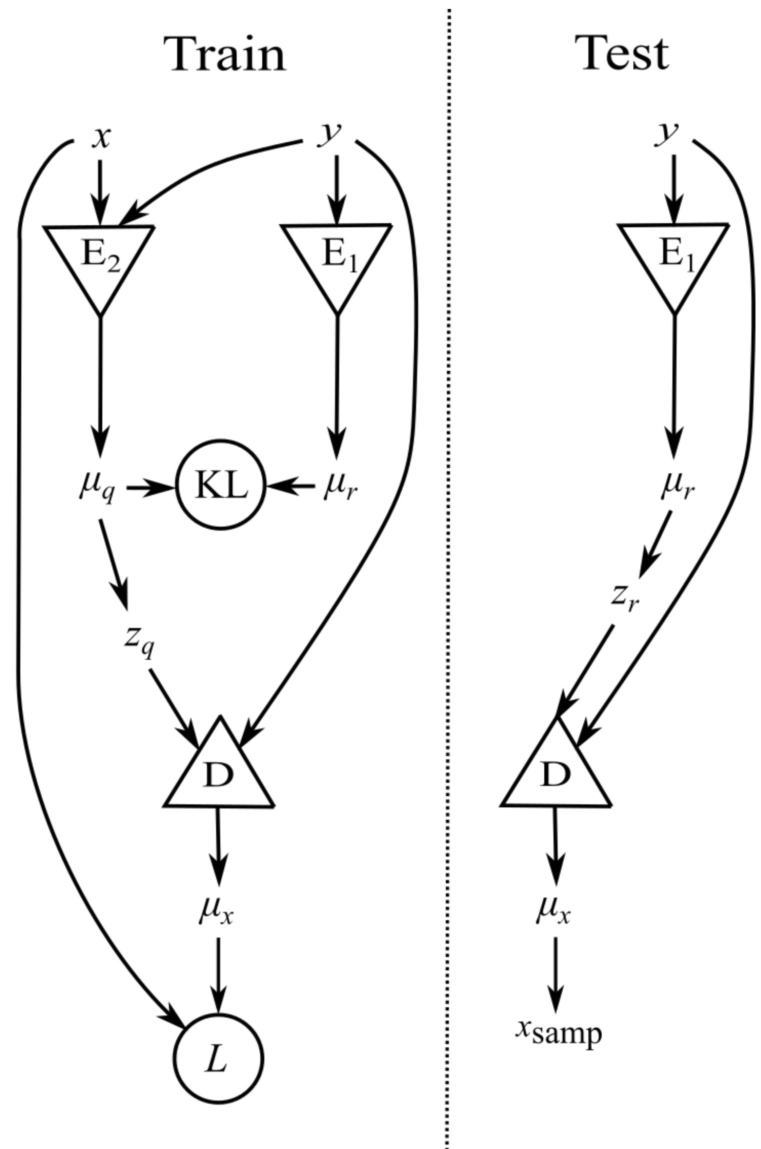

x: GW model parameters (masses, distance, etc.)
y: Corresponding GW strain data
L: Reconstruction loss
KL: Kullback-Leibler Divergence (Latent loss conditioned on specific labels)
Cost function = L + KL

Gabbard et al. 2019

Parameter estimation with CVAE

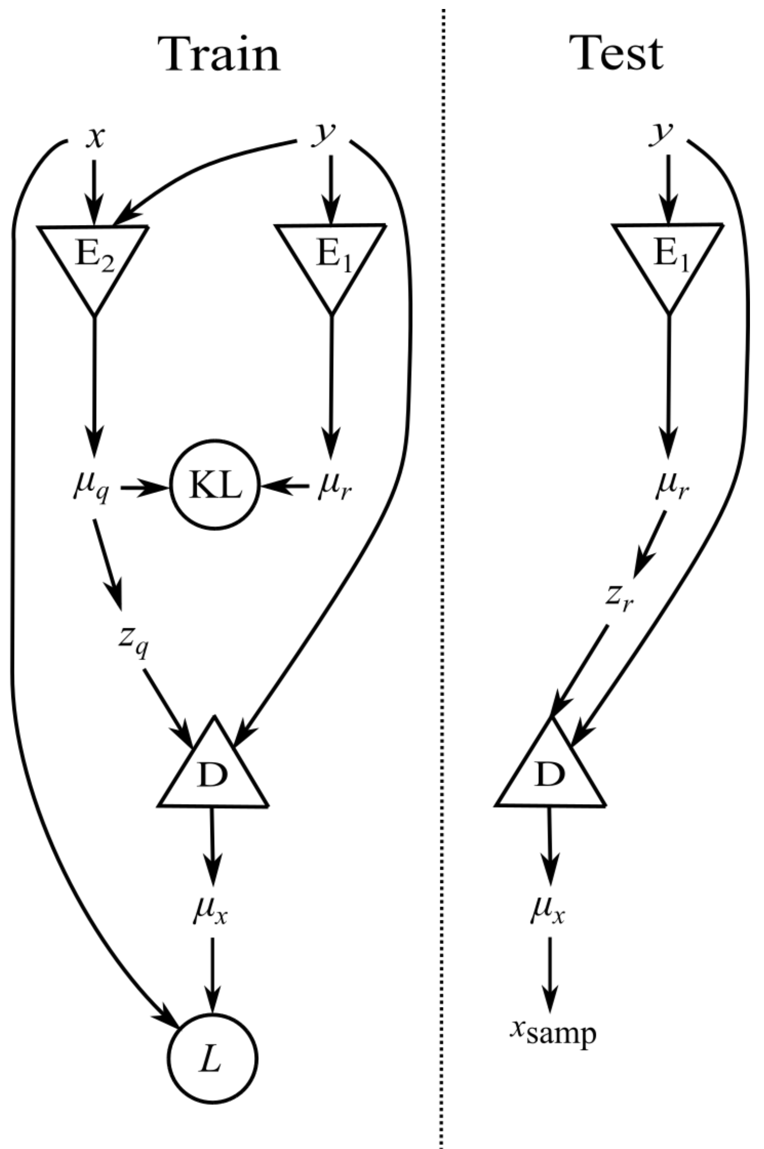

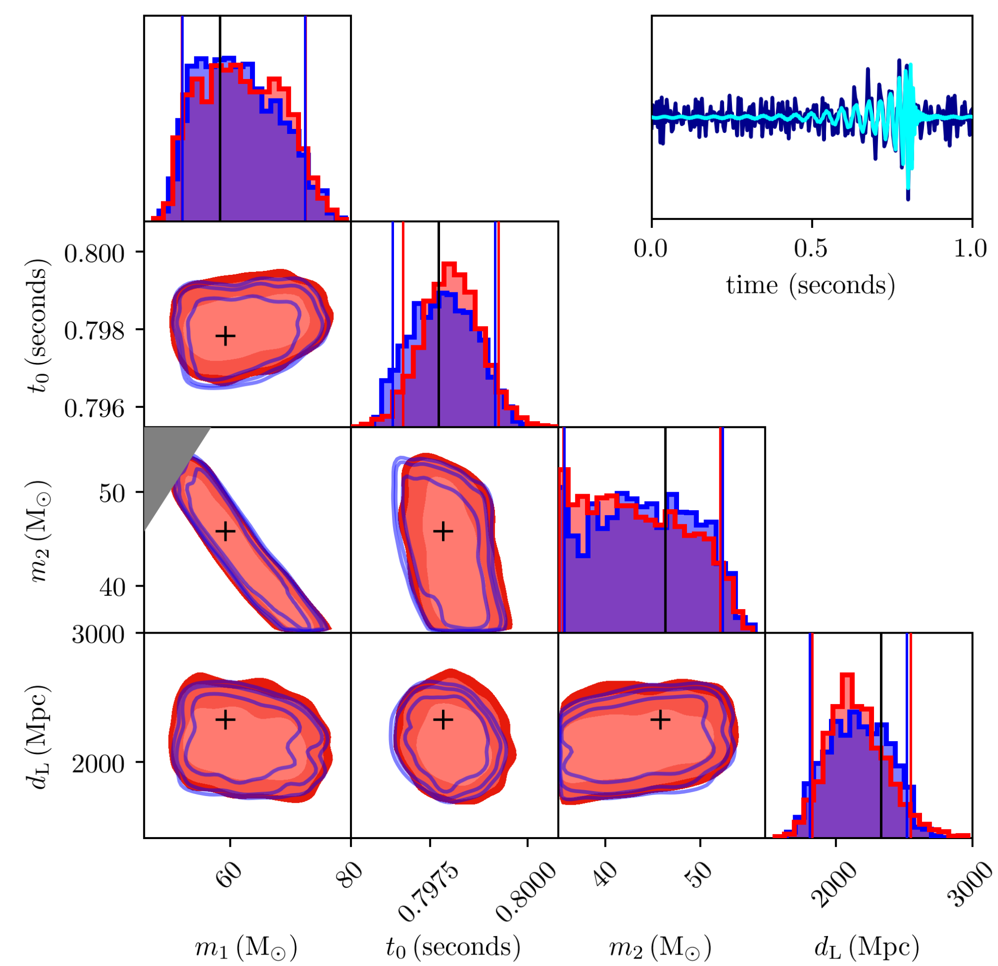

x: GW model parameters (masses, distance, etc.)
y: Corresponding GW strain data
L: Reconstruction loss
KL: Kullback-Leibler Divergence (Latent loss conditioned on specific labels)
Cost function = L + KL

Gabbard et al. 2019

Parameter estimation with CVAE

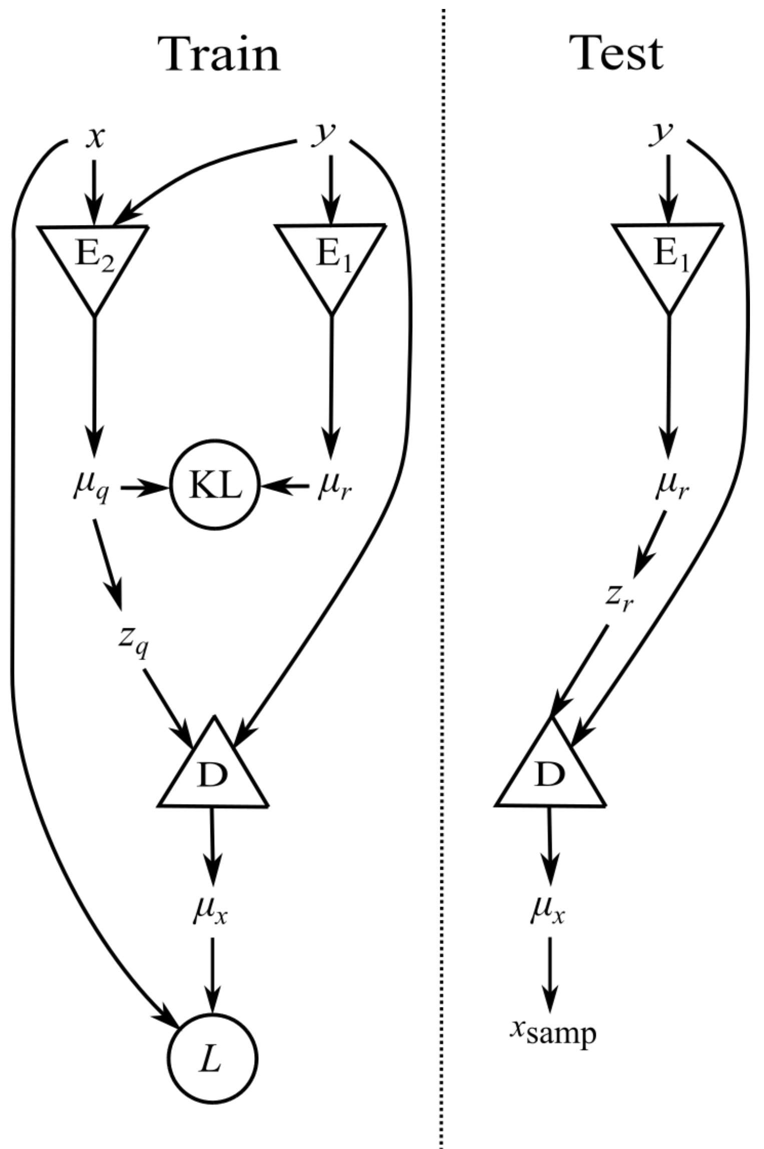

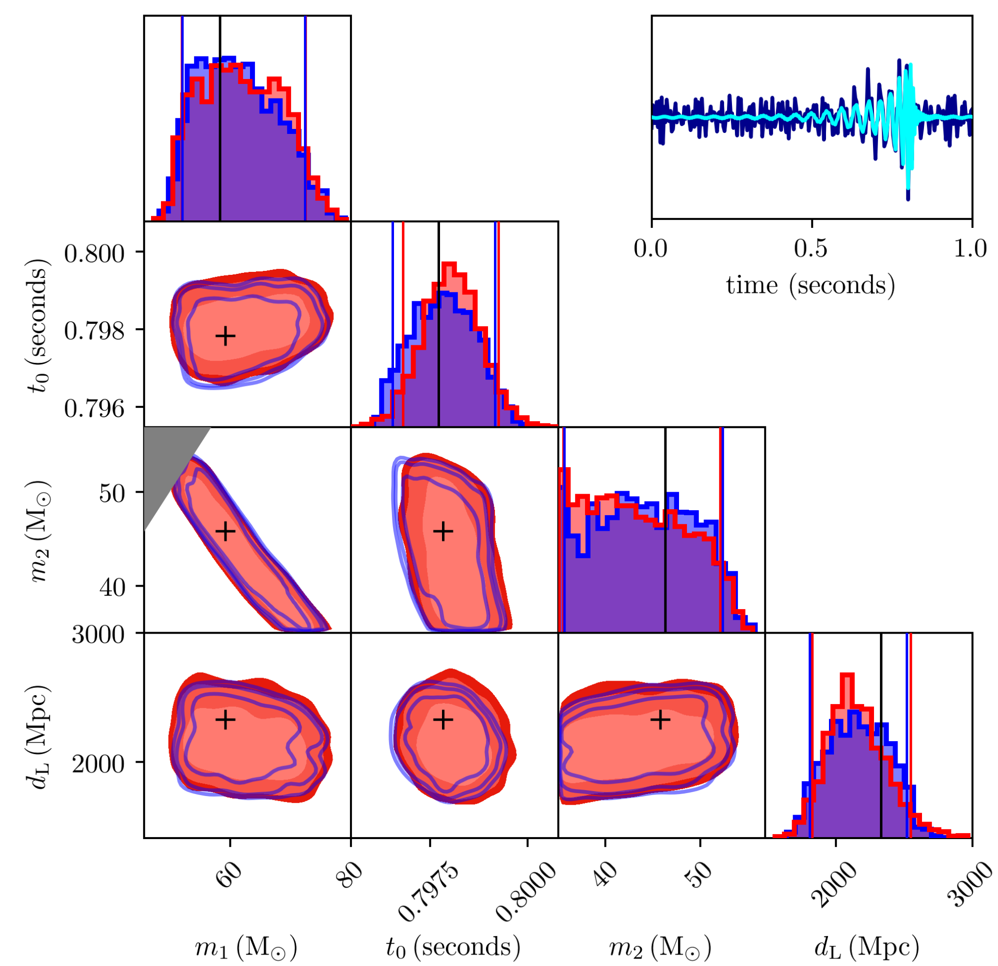

x: GW model parameters (masses, distance, etc.)
y: Corresponding GW strain data
L: Reconstruction loss
KL: Kullback-Leibler Divergence (Latent loss conditioned on specific labels)
Cost function = L + KL

Posterior distributions for 1 example dataset
Red: CVAE, Blue: Bayesian code (Bilby+dynesty sampler)

Gabbard et al. 2019

Parameter estimation with CVAE

Gabbard et al. 2019

Parameter estimation with CVAE

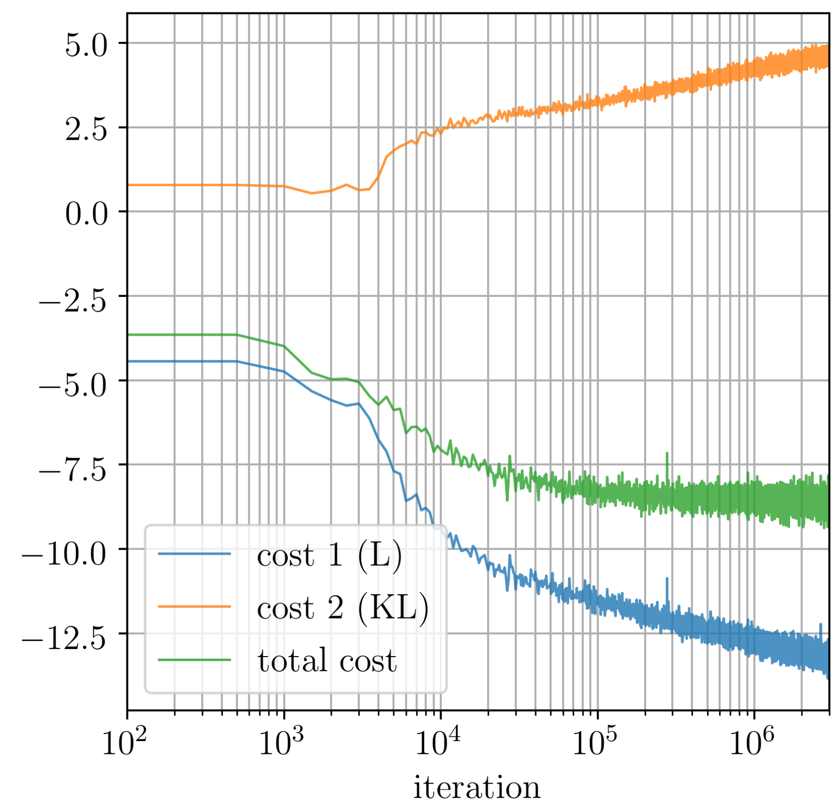

Gabbard et al. 2019

Parameter estimation with CVAE

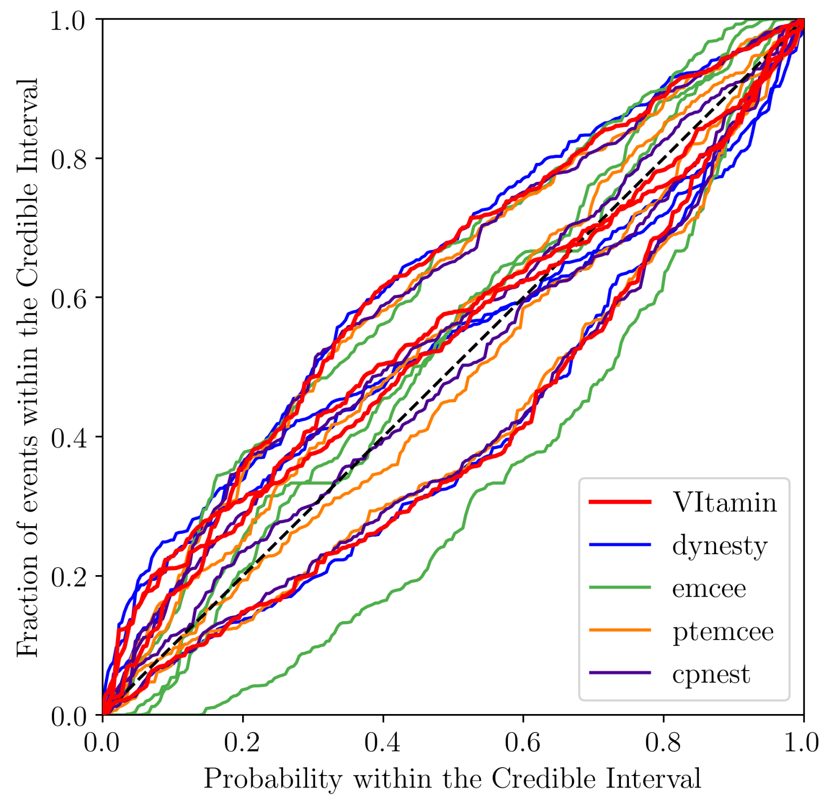

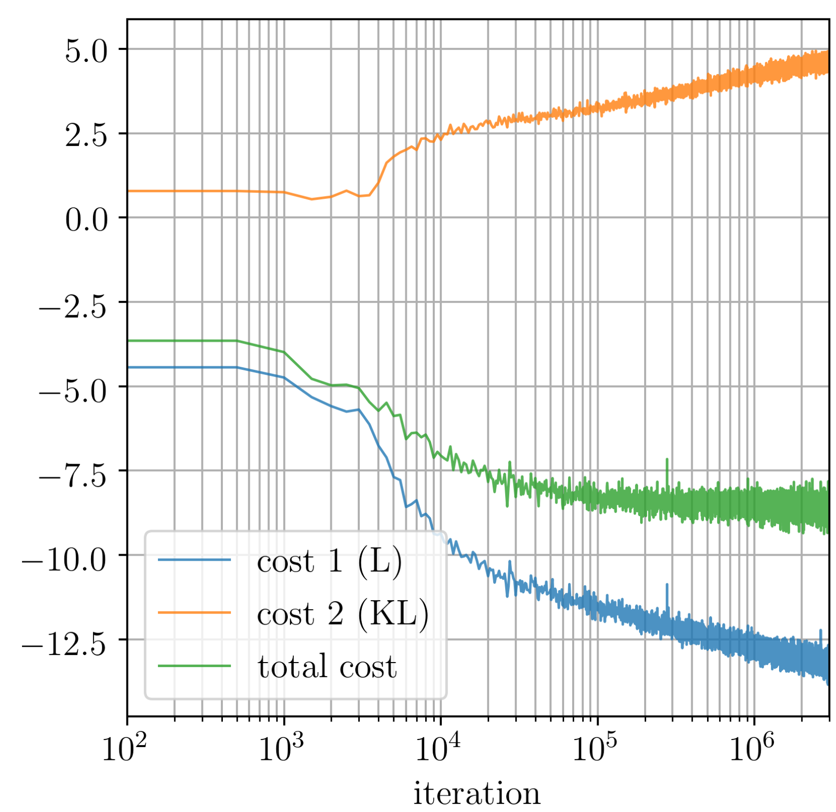

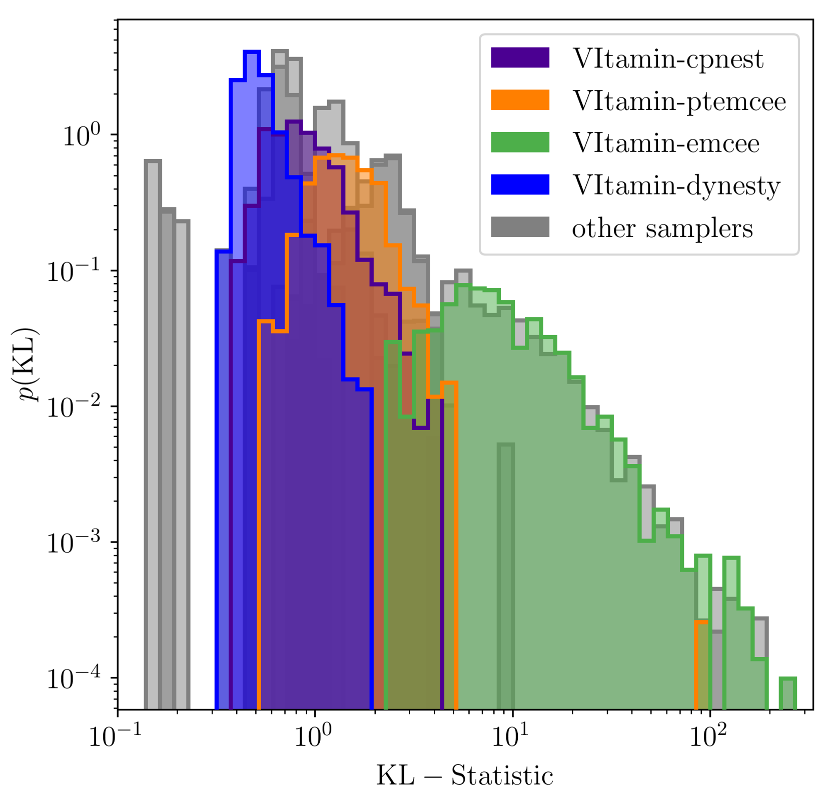

Gabbard et al. 2019

Parameter estimation with CVAE

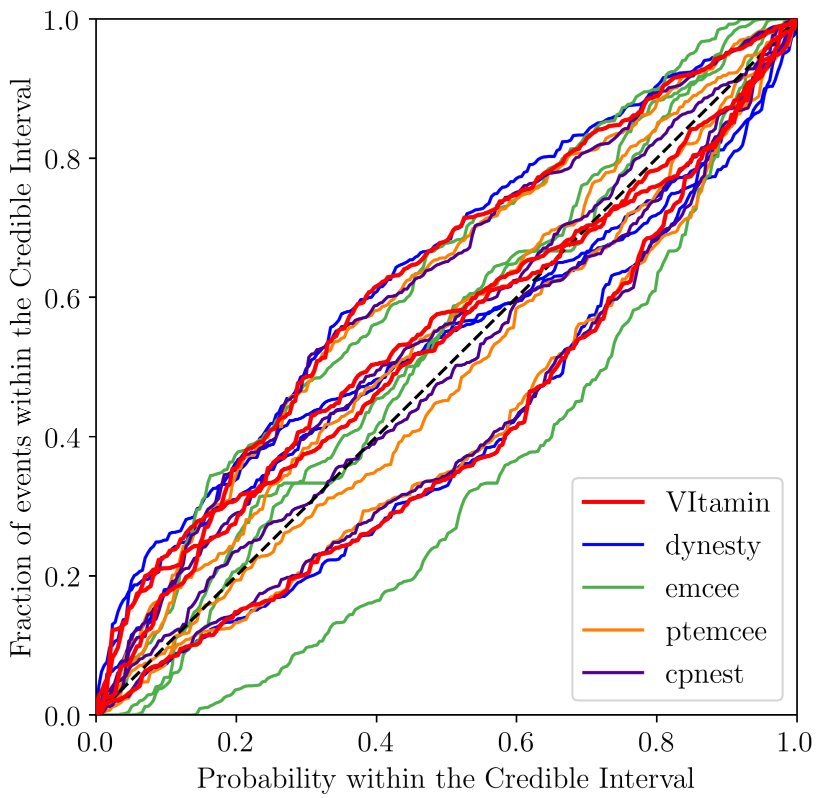

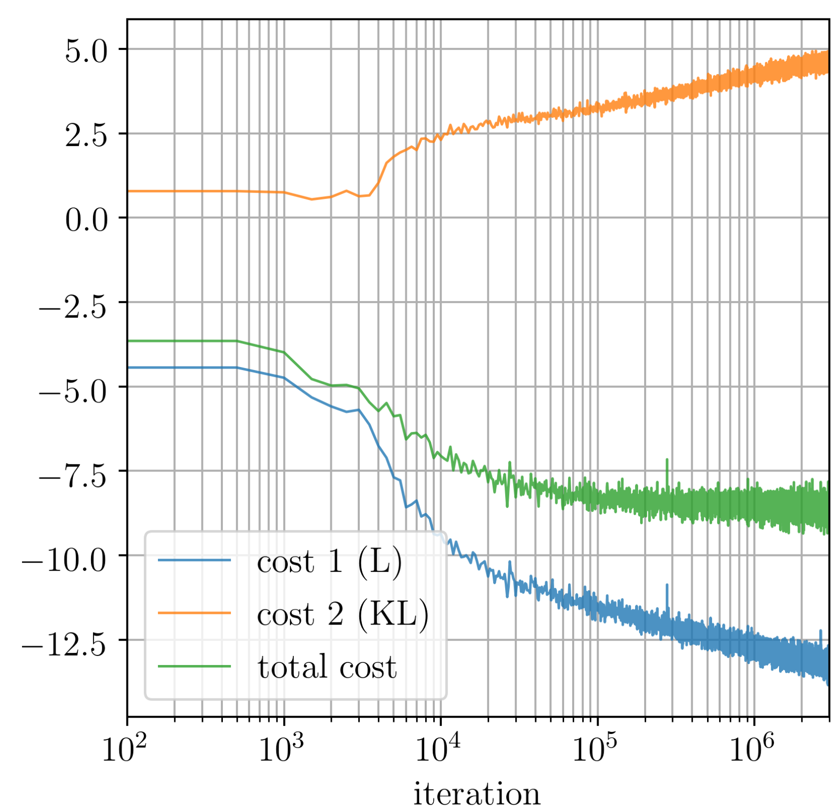

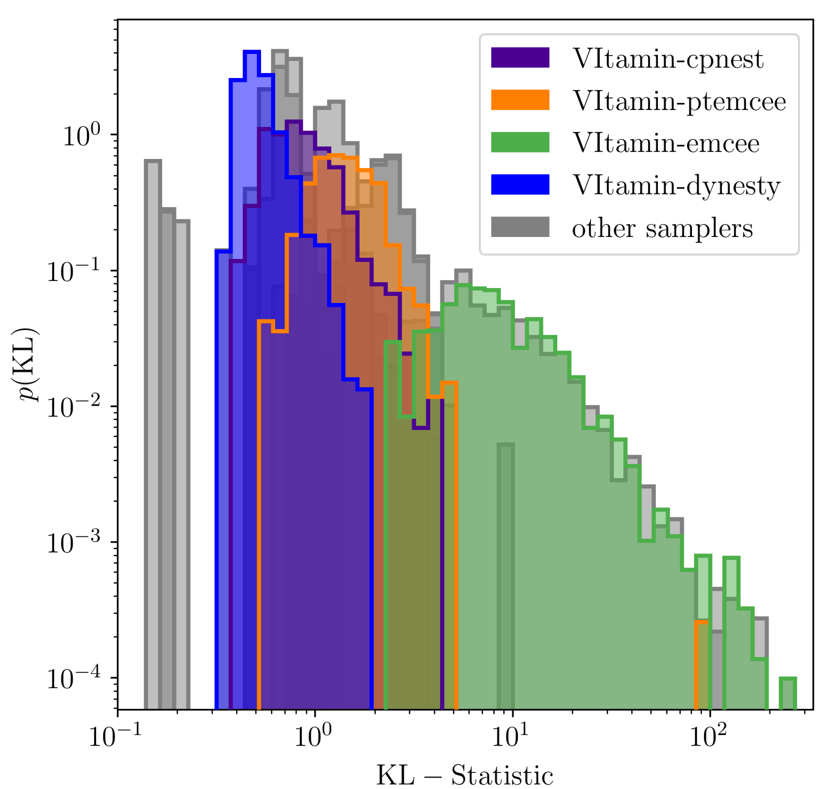

TABLE I. Durations required to produce samples from each of the different posterior sampling approaches.

sampler	run time (seconds)			ratio $\frac{\tau_{\text{VItamin}}}{\tau_X}$
	min	max	median	
Dynesty[a]	602	1538	774[b]	2.6×10^{-6}
Emcee	2005	11927	4351	4.6×10^{-7}
Ptemcee	3354	12771	4982	4.0×10^{-7}
Cpnest	1431	5405	2287	8.8×10^{-7}
`VItamin`[c]	$\mathbf{2 \times 10^{-3}}$			1

Gabbard et al. 2019

Parameter estimation with Deterministic and Bayesian NN

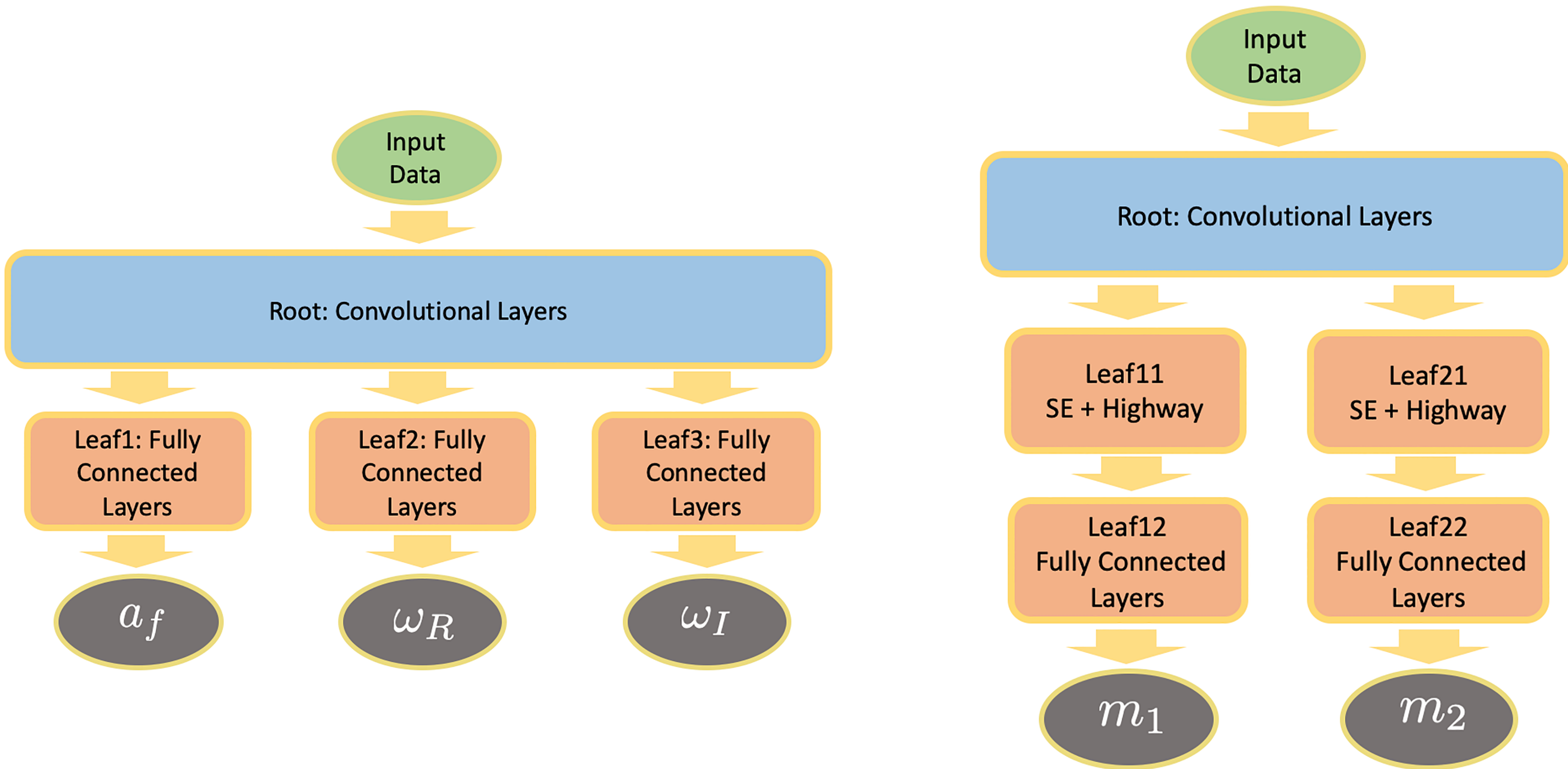

FIG. 1. The left architecture is used to estimate the final spin and quasi-normal modes of the black hole remnant. The right architecture is used to estimate the masses of the binary black hole components.

- Realistic BBH scenarios used to generate 10^7 waveforms:
  - spins are (anti-)aligned
  - evolve on quasi-circular orbits
- Both NNs are fully trained and used in parallel for inferences studies
- Parameters of BBH mergers constructed within 2 milliseconds using a single Tesla V100 GPU

Shen et al. 2019

Results of Bayesian NN models

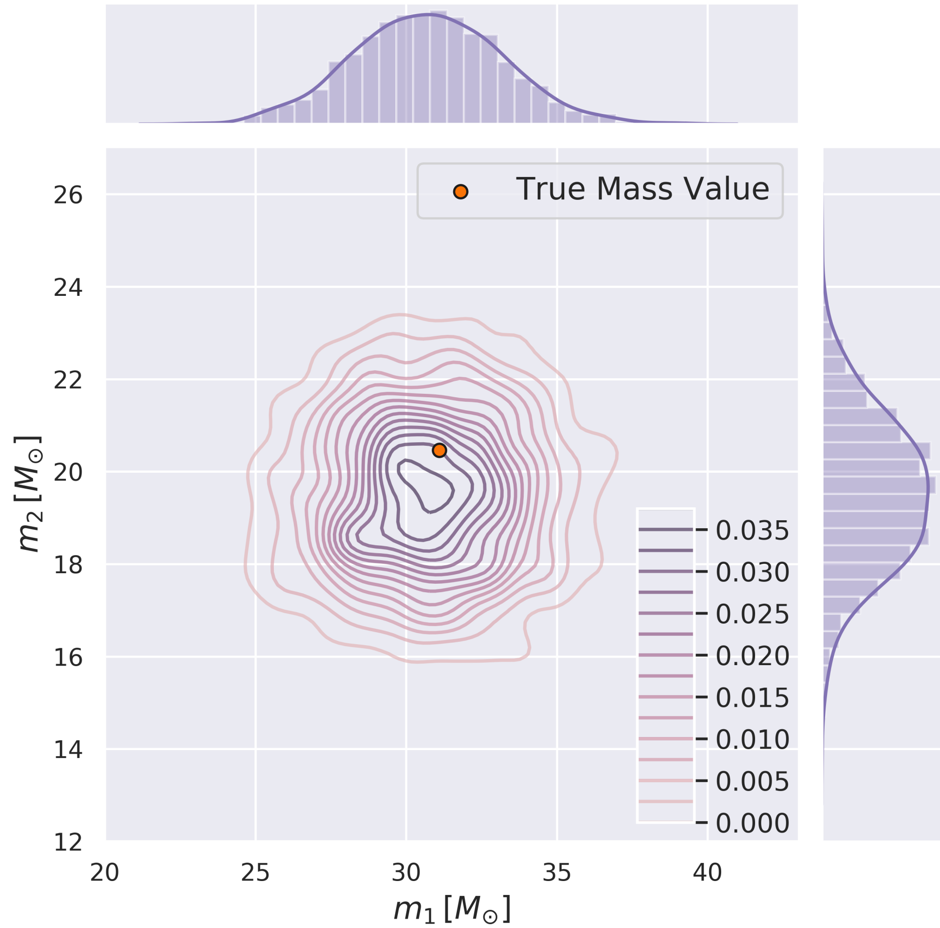

(a)SNR = 13.0

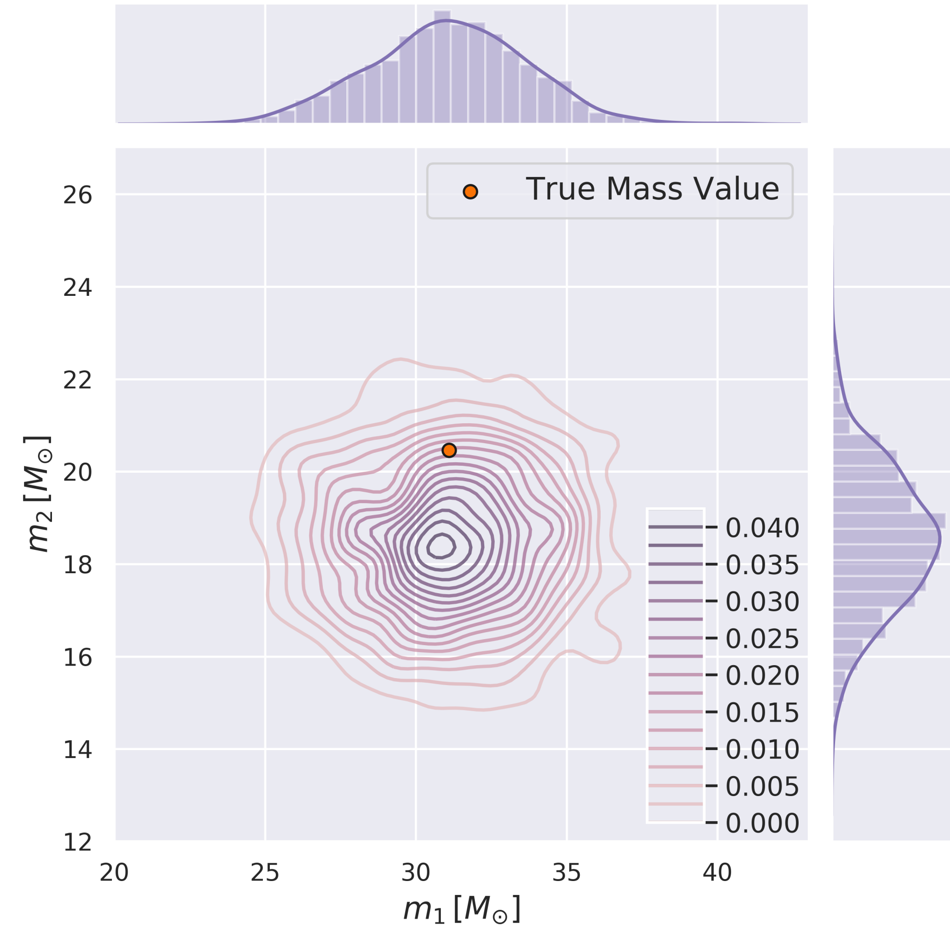

(b)SNR = 19.5

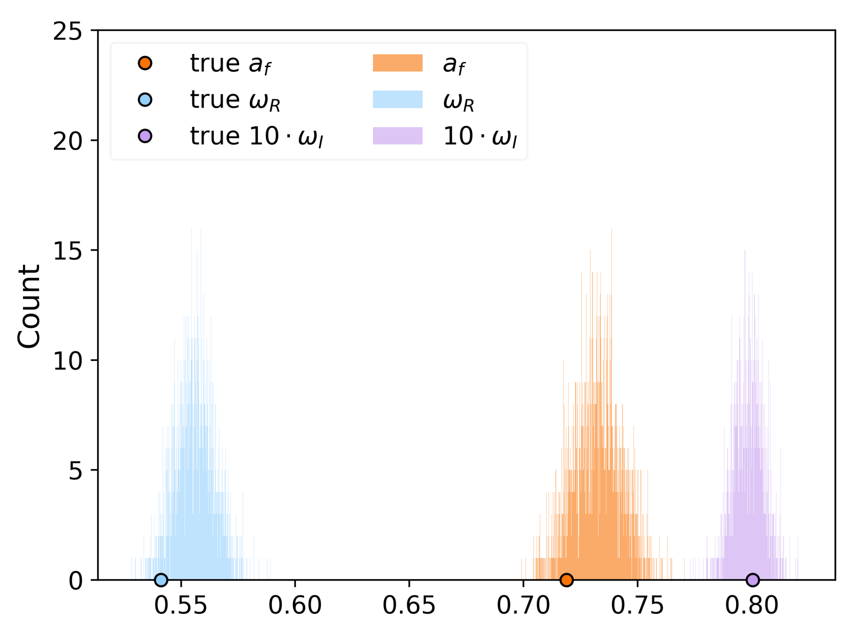

(c)SNR = 13.0

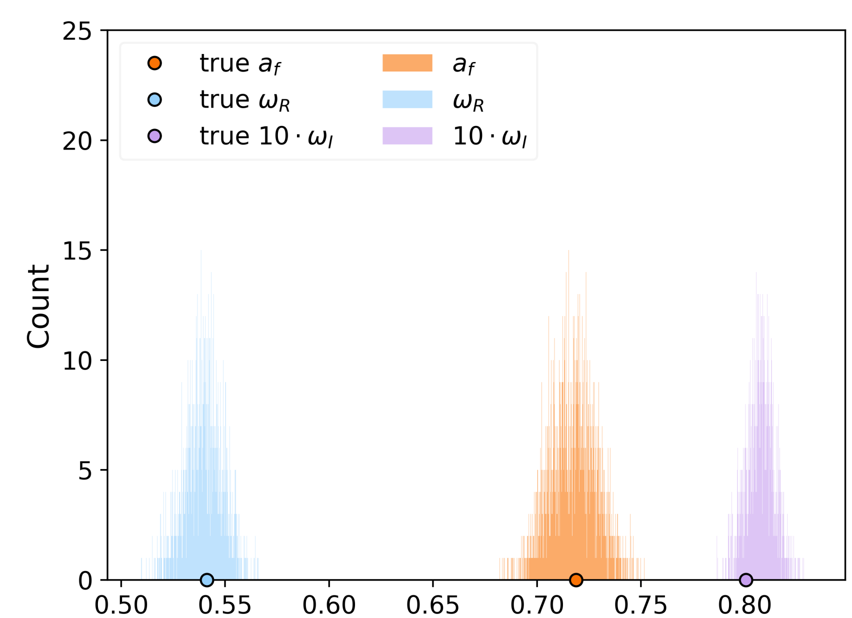

(d)SNR = 19.5

Shen et al. 2019

Localisation of GW sources with ANN

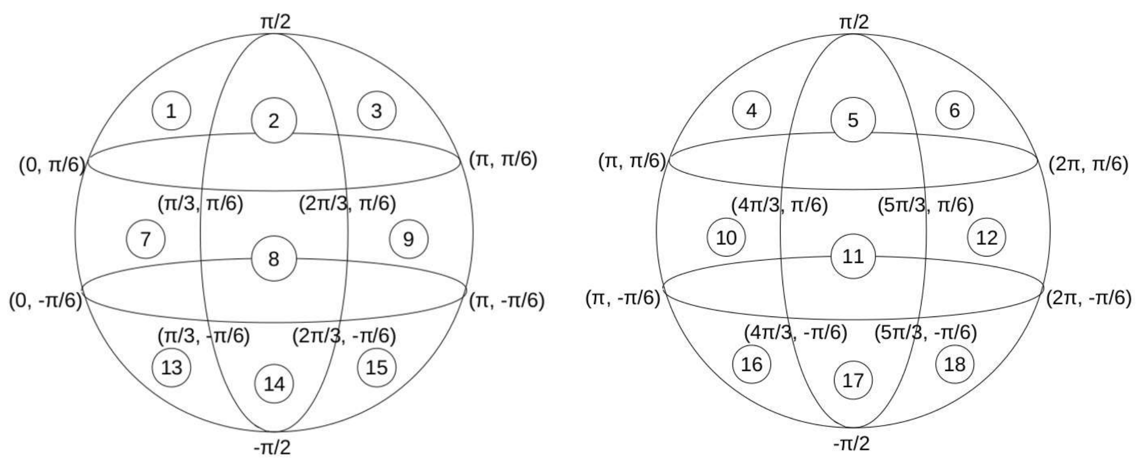

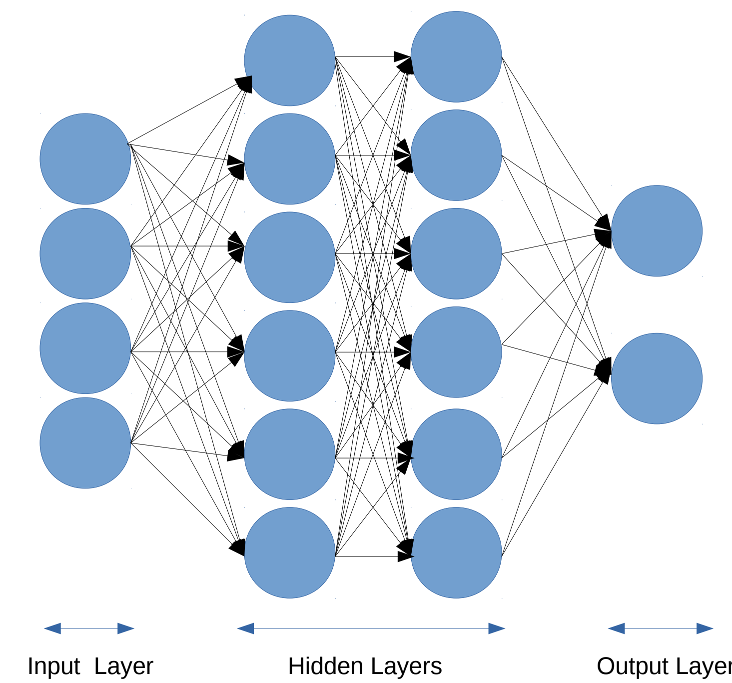

- Set up an ANN which will attempt to identify the correct sector in the sky in order to locate the origin of GW source
- Input features used are the delays in arrival times, phase differences and amplitude ratios and cross-correlations
- These inputs are computed at each of the three detectors using the signals with and without noise

Chatterjee et al. 2019

Localisation of GW sources with ANN

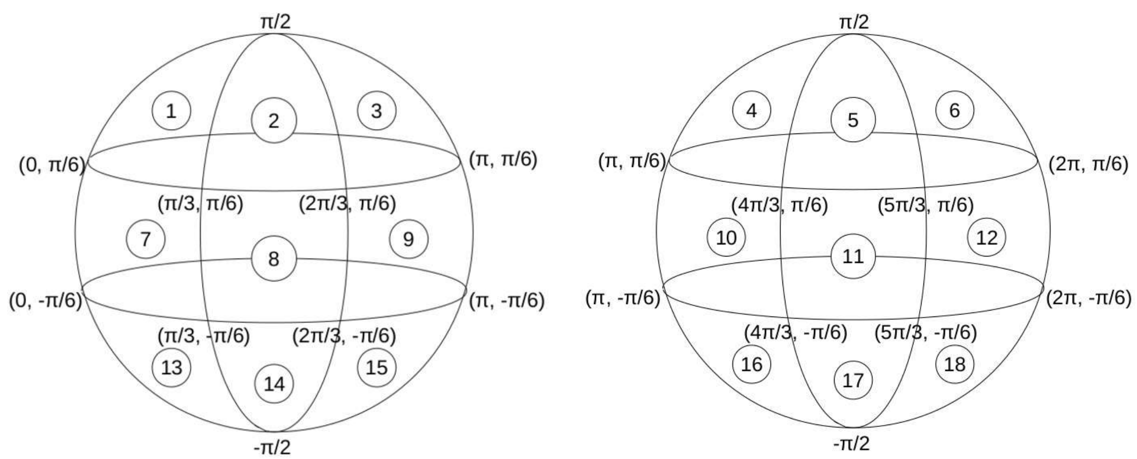

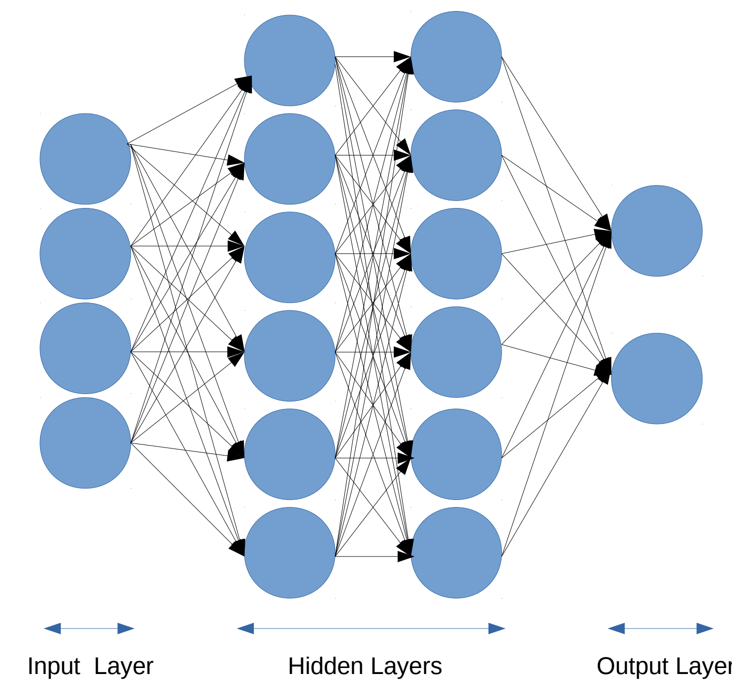

- Set up an ANN which will attempt to identify the correct sector in the sky in order to locate the origin of GW source
- Input features used are the delays in arrival times, phase differences and amplitude ratios and cross-correlations
- These inputs are computed at each of the three detectors using the signals with and without noise

Table IV. Results for pure signals and coarse angular resolution. Training with 10800 samples, tested with 1200 samples. Batch size = 250, number of epochs = 300.

Number of sectors	Training accuracy	Test set accuracy
18	98%	95%
50	97%	91%
128	95%	85%

Chatterjee et al. 2019

Localisation of GW sources with ANN

Table V. Results for signals plus Gaussian noise and coarse angular resolution. Trained with 160000 samples, validated with 40000 samples, tested with 4000 samples. Batch size = 2000.

SNR	Number of sectors	Training accuracy	Test accuracy	Revised test accuracy[a]
[50-55]	18	89%	91%	98.5%
[50-55]	50	80%	84%	98.25%
[50-55]	128	70%	77%	97.8%
[20-35]	18	80%	85%	97.27%
[20-35]	50	69%	73%	96%
[20-35]	128	55%	62%	92%
[10-110][b]	128	60%	65%	94.5%[c]

[a] correct within one sector
[b] With Curriculum Learning
[c] Tested on samples with SNR of [20-35]

Chatterjee et al. 2019

Localisation of GW sources with ANN

Table V. Results for signals plus Gaussian noise and coarse angular resolution. Trained with 160000 samples, validated with 40000 samples, tested with 4000 samples. Batch size = 2000.

SNR	Number of sectors	Training accuracy	Test accuracy	Revised test accuracy[a]
[50-55]	18	89%	91%	98.5%
[50-55]	50	80%	84%	98.25%
[50-55]	128	70%	77%	97.8%
[20-35]	18	80%	85%	97.27%
[20-35]	50	69%	73%	96%
[20-35]	128	55%	62%	92%
[10-110][b]	128	60%	65%	94.5%[c]

[a] correct within one sector
[b] With Curriculum Learning
[c] Tested on samples with SNR of [20-35]

Table IX. Areas of 50% and 90% confidence contours for our GW150914, GW170818 and GW170823 test samples with 2048 sectors.

Event	90% contour (in $\deg^2$)	50% contour (in $\deg^2$)
GW150914	312	74
GW170818	2050	354
GW170823	429	94

Tests on 3 real GW events

Chatterjee et al. 2019

Localisation of GW sources with ANN

Table V. Results for signals plus Gaussian noise and coarse angular resolution. Trained with 160000 samples, validated with 40000 samples, tested with 4000 samples. Batch size = 2000.

SNR	Number of sectors	Training accuracy	Test accuracy	Revised test accuracy[a]
[50-55]	18	89%	91%	98.5%
[50-55]	50	80%	84%	98.25%
[50-55]	128	70%	77%	97.8%
[20-35]	18	80%	85%	97.27%
[20-35]	50	69%	73%	96%
[20-35]	128	55%	62%	92%
[10-110][b]	128	60%	65%	94.5%[c]

[a] correct within one sector
[b] With Curriculum Learning
[c] Tested on samples with SNR of [20-35]

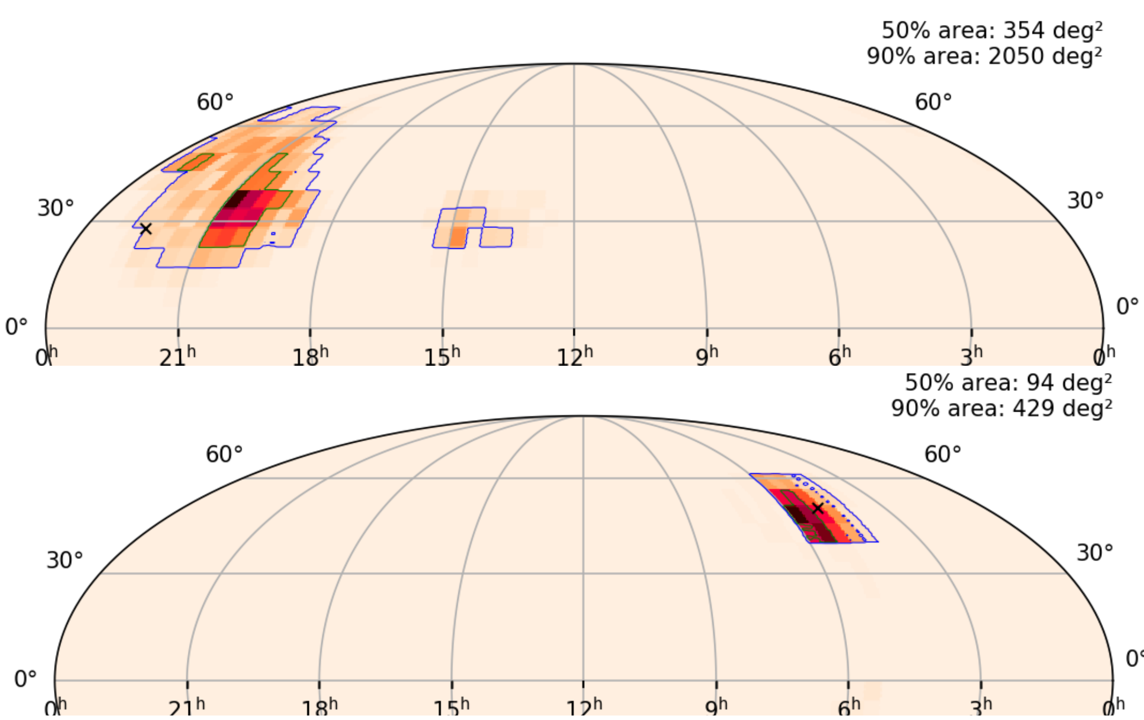

Table IX. Areas of 50% and 90% confidence contours for our GW150914, GW170818 and GW170823 test samples with 2048 sectors.

Event	90% contour (in deg^2)	50% contour (in deg^2)
GW150914	312	74
GW170818	2050	354
GW170823	429	94

Tests on 3 real GW events

Chatterjee et al. 2019

Sensing and Control

Sensing and Control

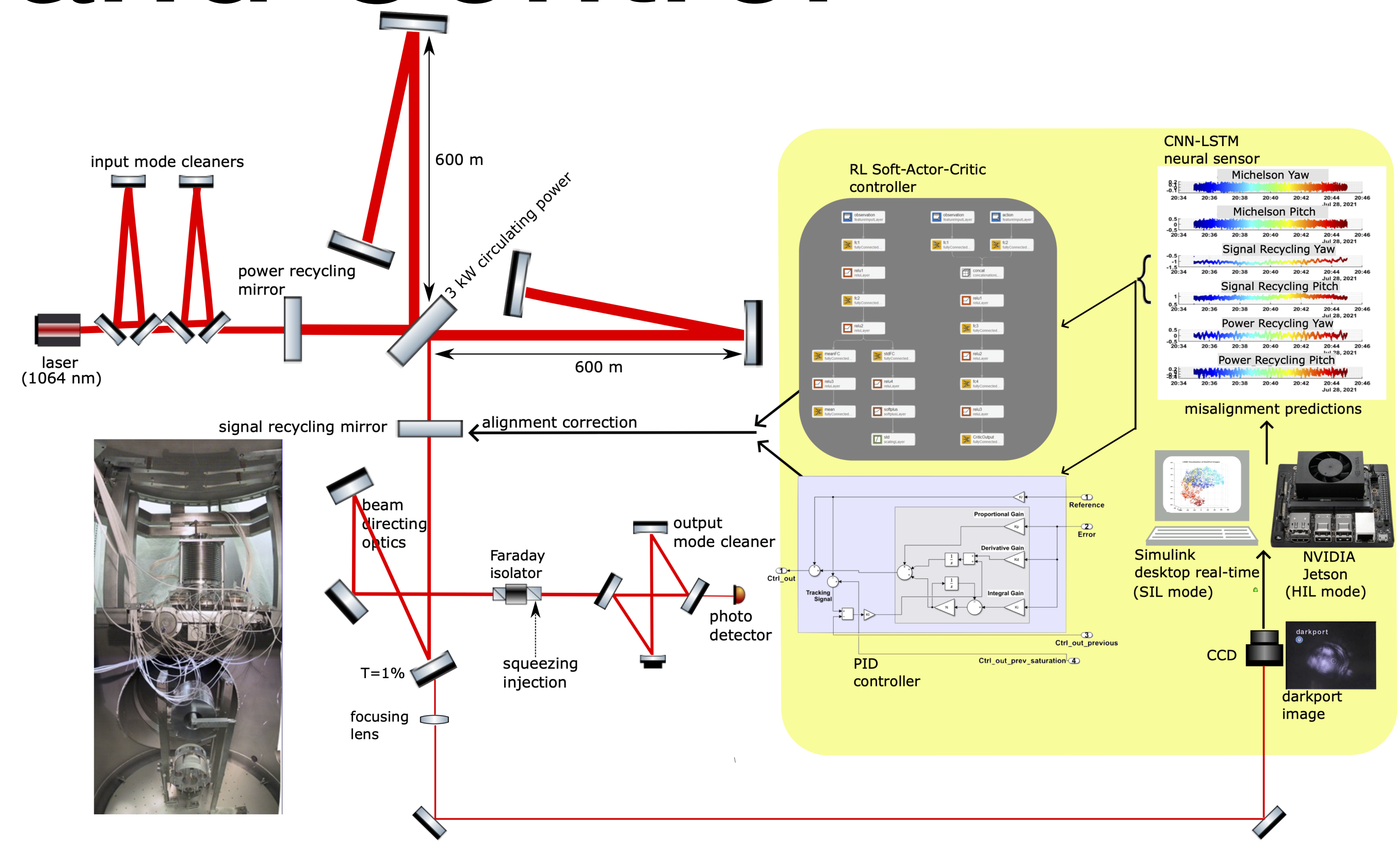

Automated alignment

Suspended optics can suffer from mis-alignment from slow drifts over time (temperatures and seismic variations) resulting in worsened sensitivity to detect signals

A network that extracts the information of the state of the interferometer and controls/ corrects it.

Sensing: Alignment information is extracted using a CNN-LSTM network

Control: Reinforcement learning - Soft-Actor-Critic controller then applies auto-alignment corrections resulting in improved sensitivity to astrophysical signals

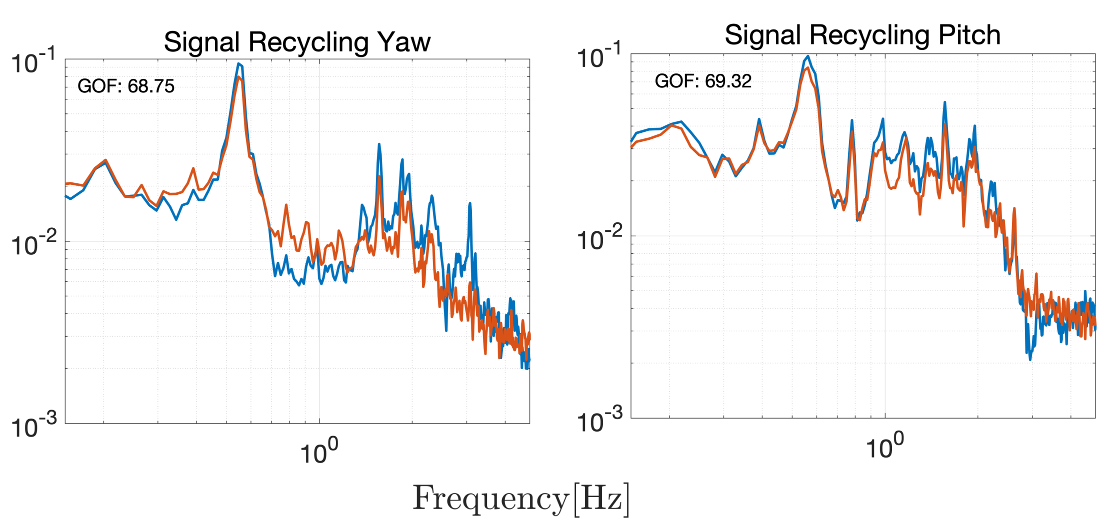

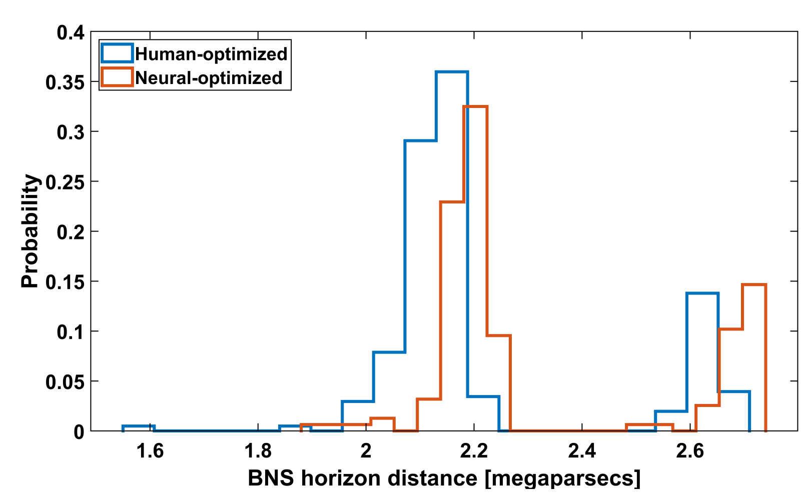

Mukund et al 2023

Language

Processing

Hey LIGO!

Information Retrieval and Recommendation system

- Hey LIGO - open access NLP-based web app *(applicable to any observatory data logs)*
- Contextual learning - Converts raw data into structured usable format
- Identify prominent keywords from logbook entries
- Use associated metadata to quantify, analyze and make useful recommendations
  - detector maintenance, glitch occurrence and correlations with time/detector/subsystems
  - applicable to any (non-GW) observatory logs

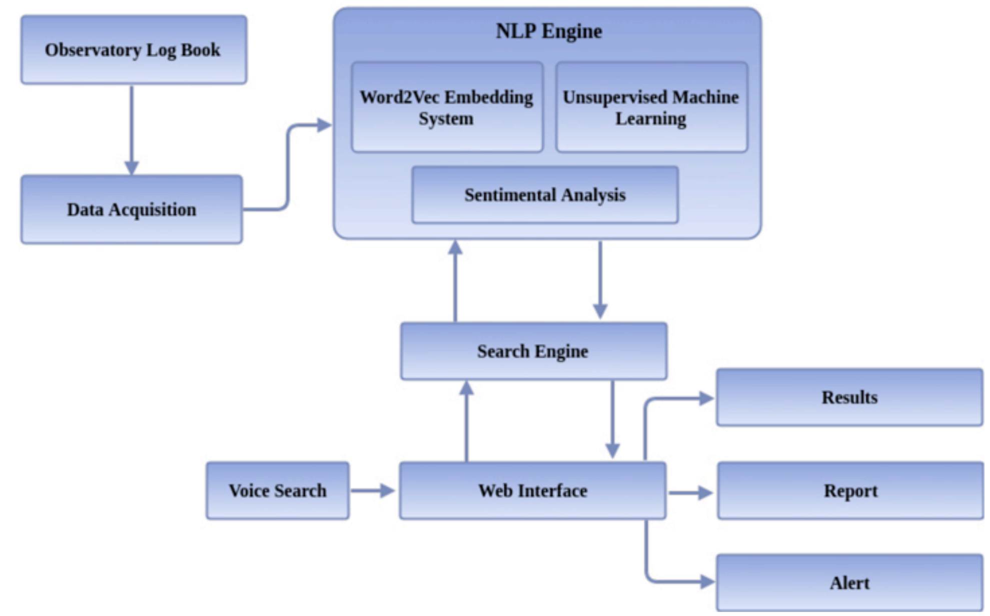

Table 2
Prominent LLO Logbook Keywords from 2017 January 1 to June 30

Keyword	Logbook Entries	Posts Retrieved by NLP Code: Total	Posts Retrieved by NLP Code: Relevant
Lock Loss	108	108	89
Earthquake	83	94	80
Charge Measurement	62	65	58
Guardian	55	65	55
Optical Lever	63	61	48
Calibration Lines	55	52	45

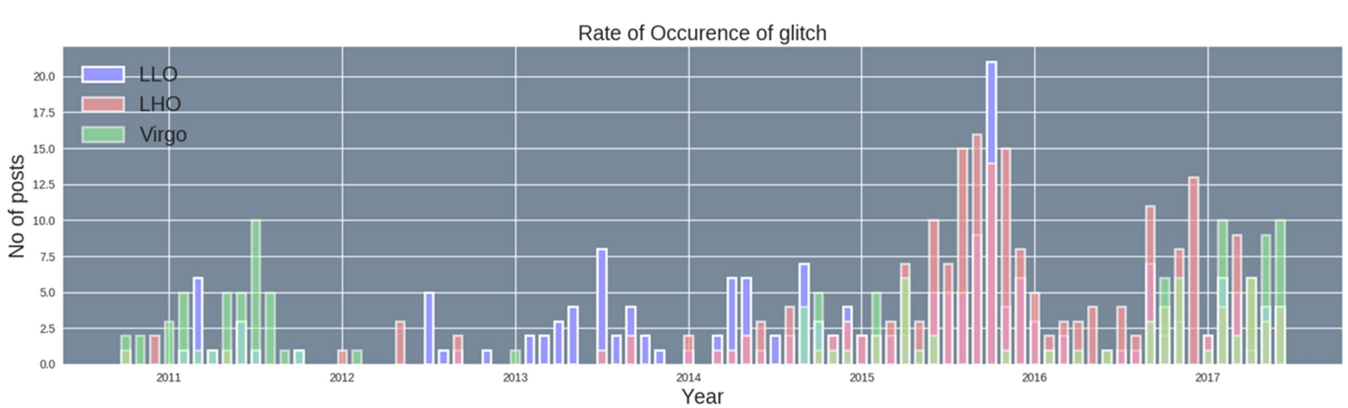

Glitch Distribution over time for three GW detectors

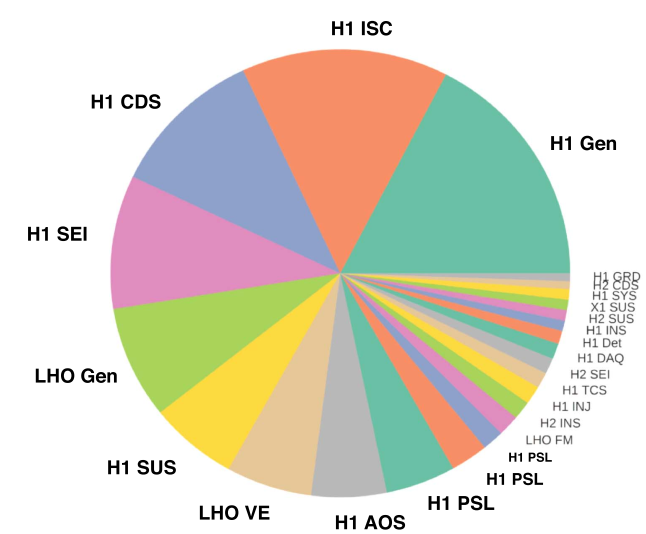

Glitch Distribution across different subsystems

Mukund et al. 2018


ML Applications in GW
Glitch identification/ characterisation
Denoising
Parameter prediction
Predictive maintenance
Signal Detection
Language processing
Waveform generation
Real time monitoring and control